MAPPING COLORED DISSOLVED ORGANIC MATTER (CDOM) OF NAIVASHA LAKE (KENYA) FROM MERIS SATELLITE IMAGERY

BASHANA WONDIMU DAKSA
March, 2011

SUPERVISORS:
Dr. Ir. C. M. M. (Chris) Mannaerts
Dr. Ir. Mhd. (Suhyb) Salama
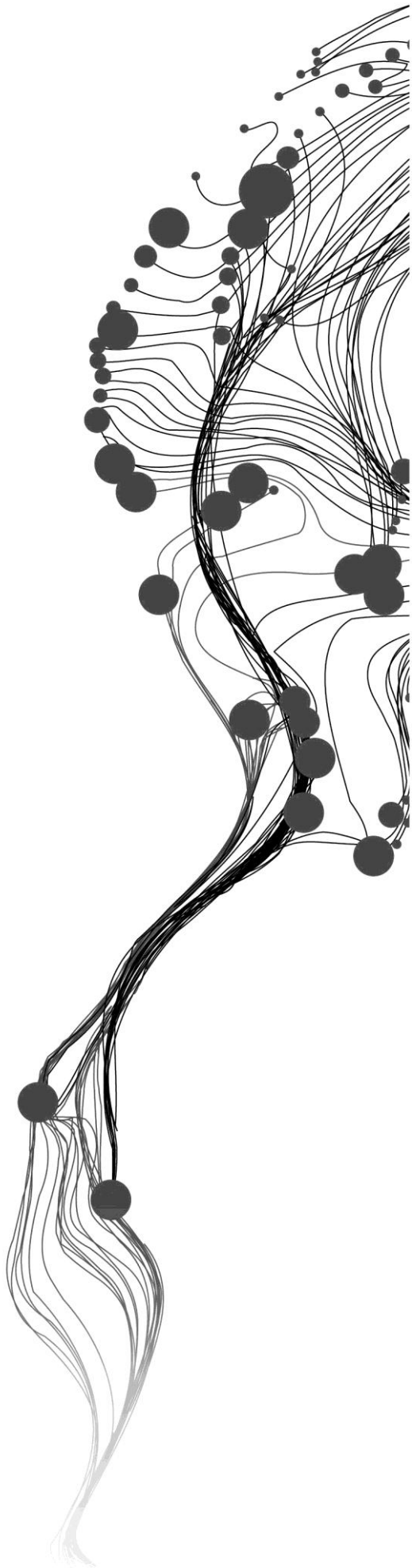
MAPPING COLORED DISSOLVED ORGANIC MATTER (CDOM) OF NAIVASHA LAKE (KENYA) FROM MERIS SATELLITE IMAGERY

BASHANA WONDIMU DAKSA

Enschede, The Netherlands, March, 2011

Thesis submitted to the Faculty of Geo-Information Science and Earth Observation of the University of Twente in partial fulfilment of the requirements for the degree of Master of Science in Geo-information Science and Earth Observation.
Specialization: Water Resources and Environmental Management

SUPERVISORS:
Dr. Ir. C.M.M. (Chris) Mannaerts
Dr. Ir. Mhd. (Suhyb) Salama

THESIS ASSESSMENT BOARD:
Prof. Dr. Ing. W. (Wouter) Verhoef (Chair)
Prof. Dr. D. M. Harper Department of Biology, Leicester University, UK (External Examiner)

ABSTRACT

Sustainable use of Lake Naivasha water and sustainable protection of its aquatic environment require water quality monitoring which are important factors to offset impacts from future development.

Colored dissolved organic matter is one of the components of water quality component along with turbidity and Chlorophyll *a*. Given its importance for the structure and function of the lake ecosystems, satellite remote sensing that could estimate the concentration of CDOM in Lake Naivasha would be highly desirable to investigate its concentration data.

In situ measurements of absorption coefficients of the lake water constituents and optical measurements were carried out at 93 sampling sites in lake Naivasha. Remote sensing reflectance measured by a hyperspectral handheld spectroradiometer was used to retrieve the ratio of CDOM to total absorption coefficients (a_{CDOM}/a_t) at 412 nm. The coefficient determination (R^2) and RMSE between in situ and retrieved from optical measurements were 0.81 and 0.05 respectively. The ratio between CDOM and total absorption coefficients in the Lake was found to vary from 0.09 (in the main lake) to 0.67 (in the Crater lake) with an average value of 0.24. Remote sensing reflectances retrieved from MERIS satellite imageries of Lake Naivasha that were acquired on 20th, 23rd and 26th September 2010 concurrently with in situ absorption measurements of total CDOM were utilized for cross validation. Values of the ratio at 412 nm retrieved from MERIS imageries correlate ($R^2 = 0.84; RMSE = 0.03$) with value of a_{CDOM}/a_t at 412 nm measured during field campaign and hence, one can simply retrieve the value of absorption coefficients of CDOM in the lake from MERIS imageries by strategic sampling and improving laboratory measurement of total absorption coefficients of the lake Naivasha by using empirical algorithm proposed for optically complex water. The spatial variability of concentration of CDOM is insignificant with average value of 4.06 ± 0.63 m^{-1} where as Absorption of particles in the lake varies between 2.30m^{-1} and 34.31m^{-1} with an average value of 14.36 m^{-1} and a standard deviation of 5.51 which confirms the large variability of suspended particles (phytoplankton and non algal particles) in the lake that influence the quality and quantity of subsurface irradiance in the Lake.

ACKNOWLEDGEMENTS

TABLE OF CONTENTS

LIST OF ACRONYMS, ABBREVIATIONS AND SYMBOLS

m.a.m.s.l	Meter above mean sea level
A	Absorbance [–]
$a_{CDOM}(\lambda)$	Absorption coefficient of Coloured Dissolved Organic Matter [m^{-1}]
$a_{NAP}(\lambda)$	Absorption coefficient of non algal particles [m^{-1}]
$a_{\phi}(\lambda)$	Absorption coefficient of phytoplankton [m^{-1}]
$a_P(\lambda)$	Absorption coefficient of suspended particles [m^{-1}]
$a_w(\lambda)$	Absorption coefficient of water [m^{-1}]
AOP	Apparent Optical Properties
C	Carbon
CO_2	Carbon dioxide gas
HCO_3^-	Carbonate
CO	Carbon monoxide gas
R^2	Coefficient determination
CDOM	Colored Dissolved Organic Matter
CN^-	Cyanide
DSP	Data Storage with Power Pack
DOC	Dissolved Organic Carbon
DOM	Dissolved Organic Matter
$E_s(0^+,\lambda)$	Downwelling irradiance just above the water surface [$W.m^{-2}$]
$Lsky(0^+,\lambda)$	Downwelling sky radiance [$W.sr^{-1}.m^{-2}$]
ENVISAT	ENVIronmental SATellite
ESA	European Space Agency
FR	Full Resolution
IOP	Inherent Optical Properties
l	Light path length of the cuvette [m]
MERIS	MEdium Resolution Imaging Spectrometer
NAP	Non Algal Particles
N	Nitrogen
O_2	Oxygen gas
POM	Particulate Organic Matter
p	Phosphorus
PAR	Photosynthetically Active Radiation
π	Pi (3.141593)
$L_R(\lambda)$	Radiance reflected from a standard Spectralon [$W sr^{-1} m^{-2}$]
RR	Reduced Resolution
R_R	Reflectance of the diffuse reflector (Spectralon)
$R_{rs}(\lambda)$	Remote Sensing Reflectance above water surface [sr^{-1}]
RMSE	Root Mean Square Error
S	Spectral slope of CDOM [nm^{-1}]
SAM	Spectrum Acquisition Module
F	Surface Fresnel reflectance
UV	Ultraviolent light
$E_u(0^+\lambda)$	Upwelling irradiance just above the water surface [$W m^{-2}$]
$E_u(0^-,\lambda)$	Upwelling irradiance just below the water surface [$W m^{-2}$]
$L_u(0^+,\lambda)$	Upwelling radiance just above the water surface [$W sr^{-1} m^{-2}$]
λ	Wavelength [nm]
*Chl*a	Chlorophyll a

LIST OF FIGURES

LIST OF TABLES

1. INTRODUCTION

1.1. Background

Lakes are essential renewable resources for mankind and the environment. It is important for civil (water supply, irrigation, transportation), industrial (processing and cooling, energy production, fishery) and recreational purposes (Giardino et al., 2007); however, they are susceptible to eutrophication, salinisation and heavy metal contaminations due to anthropogenic influences and contribution of inflowing rivers or small and seasonal streams to nutrient enrichment from bordering land. In combination with the complex hydrological situation, highly contrasted structures evolve in time and space in these aquatic environments. Sustainable use of these water resources and sustainable protection of its aquatic environment require water quality monitoring which are important practices to offset impacts from future development and preserve the health of the human and ecosystem.

1.2. Problem Definitions

Ecology of the Lake Naivasha basin has been subjected to dramatic changes caused by excessive use of water and its catchment area by man over the last three decades (Harper, 2006). The River Malewa basin is under serious threat due to unsustainable land use practices: deforestation, siltation, increased abstraction of water and pollution by agrochemicals used by farmers along its course. This is evidence that the water output of the river from this catchment is decreasing and the water quality is not getting better that has serious implications for the social, economic and environmental health of the river basin and Lake Naivasha. Overgrazing and tilling of its catchment lead to erosion (Everard and Harper, 2002) and hence, inflowing rivers contribute to nutrient enrichment. Runoff from intensive horticultural industry is also a source of nutrients and pesticides (Harper, 2006; Kitaka et al., 2002).

Colored dissolved organic matter (CDOM) in the Lake Naivasha may have several distinct sources: riverine sources (terrestrial soils), wetland (terrestrial plants), biological production (phytoplankton, zooplankton, microbial), and sediments. The significant impacts of land use on the quality and quantity of dissolved organic matter (DOM) loadings to receiving waters (Stedmon et al., 2006) and seasonal variability with freshwater runoff (Stedmon and Markager, 2005) postulate that the increasing development of the land surrounding the Lake Naivasha is a major source of CDOM with seasonal variability of concentrations and characteristics.

Supplementary justification is that CDOM optical properties are found to be inversely correlated with salinity. These strong linear relationships can be used as indication tool for monitoring CDOM concentration in the Lake water (Nieke et al., 1997). Terrestrial origin CDOM largely consists of a variety of polymers derived from the degradation of terrestrial and aquatic plant materials' excretion and grazing (Kirk, 1994; Steinberg, 2003) which enter the Lake via rivers and runoff (Harvey et al., 1984). Salinity is inversely related to water bodies that are strongly affected by river input indicating a terrestrial origin for CDOM and the absence of strong in situ sources and sinks (Blough and Del Vecchio, 2002). This leads to the assumption that CDOM concentration load is elevated in the Lake in view of the facts that the Lake is fresh due to inflow from three perennial river systems, and smaller and seasonal streams into the Lake (Becht and Harper, 2002).

Fresh water from the rivers influences the concentration and distribution of nutrients and biochemical elements; thus giving rise to a complex ecosystem. Lake Naivasha experiences fluctuating water levels (Vincent et al., 1979) which influence its area, limnology and hence productivity. Human induced changes have increased nutrient concentrations, and this has affected phytoplankton biomass, so that the lake was

considered moderately eutrophic (Kilham and Kilham, 1990) before 20 years; however, Ballot et al. (2009) recently found that the Lake shifted to higher trophic conditions according to the classification system for warm water tropical lakes (Salas and Martino, 1991). The effects of eutrophication and increased exploitation of water resources lead to the need to understand CDOM in order to accurately predict the effects of any changes. In shallow eutrophic lakes there is high formation of CDOM by algae, high influx of allochthonous CDOM and resuspension of CDOM by lake sediments (Laanen, 2007). Moreover, effective approaches that can fulfil the needs for its spatial and temporal monitoring are critical in the Lake. The collection of in situ data with traditional techniques may not be sufficient to acquire an understanding of the characteristics of target area where the water quality conditions can be changed rapidly as a consequence of blooms or meteorological conditions (Giardino et al., 2010); therefore, remote sensing offer a satisfactory response to the challenge.

The call for this work is to provide synoptic satellite estimates of CDOM that promotes for understanding of aquatic ecosystem, development of protection and restoration strategies, and establishment of water quality targets (Corbett et al., 2007) with the aim of upholding healthy under the Lake ecosystem.

Determination of inherent optical properties (IOPs) needs better insight of CDOM pool because it influences the accuracy of satellite based measurements of chlorophyll due to its impact upon underwater light field (Nelson and Siegel, 2002).

Remote sensing of inland waters is quite challenging due to the complicated signals from turbid water, bottom reflectance (when visible) and adjacent land surfaces. Water system with different optically active substances with temporal and spatial variations is by far more complex and requires more sophisticated models and algorithms for remote sensing and separation of the water constituents than a system containing one component only like the ocean waters. The present combinations of sensors, models and parameterizations have not been successful to retrieve CDOM concentrations in inland waters in other than in isolated cases (Henderson, 1979) indicating the need for research to determine under which conditions CDOM can be retrieved from remote sensing observations.

The frequent use of simulated datasets in literature masks information on true retrieval accuracies. Current ecological models are not able to reproduce the correct photic depth which in turn elevated areal primary productivity estimate (Stedmon and Osbum, 2006) for the CDOM effect on light attenuation is not incorporated in the models.

None of semi analytical approaches are specifically designed to derive separately the total and CDOM absorption coefficients. These models are used to derive water quality parameters assuming known spectral dependencies of colored dissolved organic matter and detritus absorption and sediment scattering in order to limit the number of unknowns and reduce uncertainties (Lee and Carder, 2005). Nevertheless, values of these spectral shapes are related to the constituent's biogeophysical composition and are not always known; therefore, any wrongly assumed spectral shape will lead to significant alteration of the derived IOPs. On the other hand, Salama et al. (2009) showed that deriving the spectral shapes of absorption and backscattering have improved the accuracy of the derived IOPs; however, the major assumption of these inversion models (Lee and Carder, 2005; Maritorena et al., 2002; Salama et al., 2009) is that the effects of CDOM and detritus absorptions are lumped due to the similar spectral signature.

1.3.   Research Objectives

The rationale of using remotely sensed data in the assessment of CDOM is due to its cost effectiveness and the acquirement of a wealth of synoptic information on high temporal frequency. Monitoring CDOM concentration using remote sensing in conjunction with strategic in situ sampling take part in formulating the current status of CDOM conditions in the Lake Naivasha water and help in foreseeing, mitigating and even avoiding future water catastrophes if happen due to its high concentration.

The main formulated objectives of this work are to:

1. Develop an empirical algorithm to derive CDOM concentration in Lake Naivasha using MERIS Full Resolution (FR) satellite imageries.
2. Study the variability of CDOM concentration in the Lake using sets of MERIS imageries.

1.4. Research Questions

The aim of efforts is to improve the accuracy of the concentration of colored dissolved organic matter retrieved from remote sensing spectra in the lake Naivasha, shallow eutrophic inland water. This is practiced by adopting empirical algorithm that distinguishes CDOM from other lake water constituents by trustful measurement of CDOM absorption in the laboratory and by utilization of spectral bands required for the remote sensing instrument that can accurately detect CDOM concentration.

Based on the aforementioned considerations three questions were formulated:

1. Can we develop a reliable regional empirical algorithm for CDOM retrievals from MERIS spectra?
2. What is the spectral dependency of CDOM absorption in the Naivasha Lake?
3. Is there a specific cycle about CDOM dynamics in the lake Naivasha and what is the effect of the Gilgil river?
4. What is the contribution of the CDOM to the total absorption of water constituents?

1.5. Hypothesis

In particular, Medium Resolution Imaging Spectrometer (MERIS), on board Envisat-1, which combines moderately high spatial resolution (300 m×300 m for FR data) with appropriate spectral resolution in the visible and near infrared, is useful for the frequent monitoring of optically active parameter. A hypothesis of interest is developing empirical algorithm in an attempt to quantify stable results of CDOM levels of lake Naivasha water from remotely sensed data, MERIS imageries.

1.6. Thesis Outline

In order to have insight of course of this research, the basic elements of research subjects are explained well in chapter one. Chapter two provides a theoretical background of (colored) dissolved organic matter based on literature study. Data and methods under which description of study area, in situ data acquisition, regression techniques and atmospheric correction are summarized are detailed in chapter three. Chapter four presents the results and discussions of the research work. Finally, conclusion and recommendations of this research work are concluded under chapter five.

2. COLORED DISSOLVED ORGANIC MATTER

2.1. Introduction

Any aquatic compounds that contain carbon atoms are organic matter except carbonates (HCO_3^-, i.e. carbon dioxide (CO_2) dissolved in water) or cyanides (CN^- groups) whereas inorganic matter consists of suspended matter (sand, silt and clay minerals) (Laanen, 2007). Inorganic matter is dominant inside sediment plumes of discharging rivers into receiving water bodies while the aquatic environment is made up of organic matter in deep oceanic waters.

The most important measures of physical and chemical water quality in natural waters are aquatic organic matters: particulate and dissolved organic matters. Dissolved organic matter (DOM) is the fraction which passes through a filter with a 0.2 μm pore size while the particulate organic matter (POM) remains on the same filter as residue. DOM is the largest reservoir of organic carbon in the aquatic environment (Hansell and Carlson, 2002); however, it cannot be measured directly. The measured value of dissolved organic carbon (DOC) is commonly used as a substitute value for DOM. The estimation of DOM from DOC is based on the findings that some 60% of DOM consists of carbon, resulting in a positive linear relationship between DOM and DOC.

Another way of technique to estimate the DOM concentration is based on a color characteristic that is shared by the majority of the compounds that make up DOM. Approaching 60-80% of freshwater DOM consists of colored molecules called colored dissolved organic matter (CDOM) that is optically measurable component of the DOM in water and therefore, it is proposed as an alternative proxy for DOM (Steinberg, 2003). CDOM is a key component of water quality targets along with turbidity and chlorophyll a; however, CDOM concentration and composition dynamics are not well understood, and hence, its robust concentration data investigation is a key job due to its capacity to affect benthic communities and sea grass in the water bodies under the following circumstances. These circumstances are fully detailed by Adams et al. (2009), Blough and Del Vecchio (2002), Corbett et al. (2007), Kirk (1994), McPherson and Miller (1994), Mulholland (2003), Muller et al. (2005), Obernoster et al. (2001), Singer (1999), Wells (2001) and Yee et al. (2006).

- It is a regulator of light availability due to its major light absorbing capacity, reducing the penetration 13-66% of light attenuation in the water column (impacting primary productivity). In lake environments, light absorption by CDOM protect aquatic organisms from potentially harmful radiation but can reduce the amount of PAR available for growth;
- It is photo-protective barrier against Ultraviolent (UV) radiation for seagrass beds;
- It is a regulator of oxygen demand for the reason that bacterial respiration and photochemical degradation of CDOM consume oxygen gas (O_2);
- It is a regulator of nutrient availability as it carries nutrients (C, N, and P in both inorganic & organic forms) directly and via food webs;
- It is a regulator of trace metals availability due to its ligand binding properties.
- DOM from elevated CO_2 detritus would decrease crayfish efficiency in finding food because of the higher concentration of secondary defensive chemicals present in the leachate;

In addition to its influences underwater communities, the study of DOM is the most important topics in the treatment process as it significantly influences the operations and the managements of the water treatment plants especially the disinfection units. In the disinfection process with chlorine, DOM serves as a precursor to the formation of undesirable disinfection by-products;

Different authors use different names, synonymous to CDOM: gelbstoff, yellow substance, humic substances, gilvin, aquatic humus, chromophoric dissolved organic matter.

2.2.   Characteristics of Colored Dissolved Organic Matter

The total spectral absorption coefficients of the given water samples can range from almost identical to that of pure water to unique which show orders of magnitude greater absorption than pure water especially at blue wavelengths depending on the concentrations of dissolved substances, phytoplankton and detritus. One of the goals of bio optics is to develop predictive algorithms or models for absorption curves such as those seen in Figure 9. Roughly 98% of the worlds open ocean and coastal waters fall into the Case 1 category, and almost all bio optical researches have been directed toward these phytoplankton dominated waters. However, Case 2 waters such as inland waters, near shore and estuarine are disproportionately important to human interests like recreation, fisheries, and military operations that make it to receive increasing attention in the recent years.

In limnology and soil science, the same chemicals in natural waters are commonly referred to as humic substances. Humic substances are heterogeneous compounds that constitute the major organic matrix in surface water, soil and other environmental compartments. They are negatively charged and tend to bind to heavy metals and various organic compounds (Gordon and Wang, 1994). The composition of humic substances is typically expressed in terms of its three major fractions (Kracht and Gleixner, 2000):

1. Humin: the humic substances are not soluble in water at any pH value. It is still present in natural waters in suspension though insoluble and hence, its absorption behavior contributes to the particulate organic matter absorption spectrum. A brown to black color of the filter residue for the total suspended matter measurements indicate a high humin concentration.
2. Humic acid: humic acid is the fraction of humic substances that is not soluble in water under acid conditions (below $pH = 2$), but becomes soluble at greater pH.
3. Fulvic acid: fulvic acid is the fraction of humic substances that is soluble under all pH conditions.

All these three fractions share the characteristics of being heterogeneous bio-molecules that are yellow to brown or black in color and moderate to high molecular weight. Humin it is not considered part of CDOM because it is insoluble in water. CDOM thus, is comprised of only two major fractions: humic and fulvic acids. The spectral and other characteristics of CDOM are determined by the molecular structures of humic and fulvic acids. The absorption spectrum of CDOM can be described by an exponentially decreasing function, with high absorption in the UV and blue wavelengths and almost no absorption in the red and infrared region. As the DOM molecules are also constantly interacting (on the scale of days) there is also no standard molecular structure.

The wavelengths that can be absorbed are determined by the number of electrons present in the molecule. By only absorbing part of the spectrum and transmitting the rest, molecules appear colored. In limnology and ecology another subdivision of DOM is made based on the average time between formation and subsequent degradation of DOM components (called turnover time). Two classes of DOM are identified (McKnight and Aiken, 1998).

1   Labile DOM (LDOM) which has a turnover time of hours to days;
2   Recalcitrant or refractory DOM (RDOM) which has a turnover time of weeks in months, although a fraction of RDOM has a turnover time of year because it is very resistant to micro-organisms and is mainly broken down under the influence of photobleaching.

2.3.   Sources of Colored Dissolved Organic Matter

CDOM is a mixture of compounds that are by-products of plant and animal decompositions that are emerged from both terrestrial and marine sources: peat degradation and rivers and groundwater flows, plankton and vascular aquatic plant, and anthropogenic compounds in runoff such as sewage discharge and agricultural wastes (Chen et al., 2004; Corbett et al., 2007). CDOM is classified as autochthonous CDOM and allochthonous CDOM with respect to its. Autochthonously produced CDOM is present in

Case 1 water ensuring a direct link to the phytoplankton population while it is assumed that the majority of CDOM is of allochthonous production in Case 2 waters.

2.3.1.   Autochthonous CDOM formation

Most autochthonous CDOM materials are formed in the aquatic environment by microorganisms (mostly algae) and macrophytes through secretions and autolysis of cellular contents. It is released as a result of the lyses of phytoplankton. The process of lyses is defined as the breaking down or dissolution of cells (Henderson, 1979). The decay of phytoplankton is the main source of autochthonous production of CDOM although there are several processes of formation possible; the extent of CDOM production is thus determined by the primary production. The primary production is the fixation of inorganic carbon by living organisms by the use of sunlight, producing organic compounds.

2.3.2.   Allochthonous CDOM formation

Allochthonous CDOM is composed largely of humic substances of terrestrial plant origin by means of humification (transformation of organic matter into humus). Aquatic humic substances in freshwater ecosystems are primarily of terrestrial origin. Allochthonous CDOM is formed mainly by biological degradation of terrestrial plant cell matter. In the topsoil, humification of leaf litter takes place by macrofauna, fungi or bacteria, decomposing all plant components, including lignin, into smaller and simpler compounds (Gordon and Wang, 1994; Kracht and Gleixner, 2000). These simpler organic compounds can then be recycled by serving as food for other soil organisms. Groundwater or surface runoff, however, transports a portion of the soil organic matter into the surface water. In the case of groundwater as the agent, the organic matter ending up in the lake is often the more refractory, because the more labile components are filtered out along the route. In natural inland waters the CDOM comprises mostly of fulvic acids that originate from nearby soils (Keith et al., 2002; McKnight and Aiken, 1998).

2.4.   Sinks of Colored Dissolved Organic Matter

Aiken et al. (1985) describe the degradation of CDOM as losses of dissolved humic substances from the water column via the following:

- Consumption of CDOM by bacteria
- Grazing of CDOM by phytoplankton
- Adsorption to sinking particles
- Photodegradation under the influence of UV radiation

Its decomposition under the influence of UV radiation releases carbon in the form of CO_2 and carbon monoxide (CO) (Chuanmin et al., 2006) and hence, it is significant to the global carbon cycle and climate change (Hansell and Carlson, 2002).

3. DATA AND METHODS

3.1. Study Area

3.1.1. Location

Lake Naivasha is the largest freshwater lake in the Kenyan Rift Valley, lying 80 km Northwest of Nairobi, outside the town of Naivasha. The name is derived from the local Maasai name Nai'posha, meaning "rough water" because of the sudden storms which can arise. It is situated on the floor of the Eastern Rift Valley at its highest elevation of 1886.5 meters above mean sea level (m.a.m.s.l.) with central geographical coordinates of 0°45'0" S and 36°20'0" E. East African railway and main road in the west region of the country are the main access route to the area. The lake consists of the main lake and a smaller Crater Lake Game Sanctuary.

The Name Naivasha is very famous for much of the negotiations of the Comprehensive Peace Agreement ending the Sudanese Civil War signed finally on 9th January 2005, commonly known as the Naivasha Agreement.
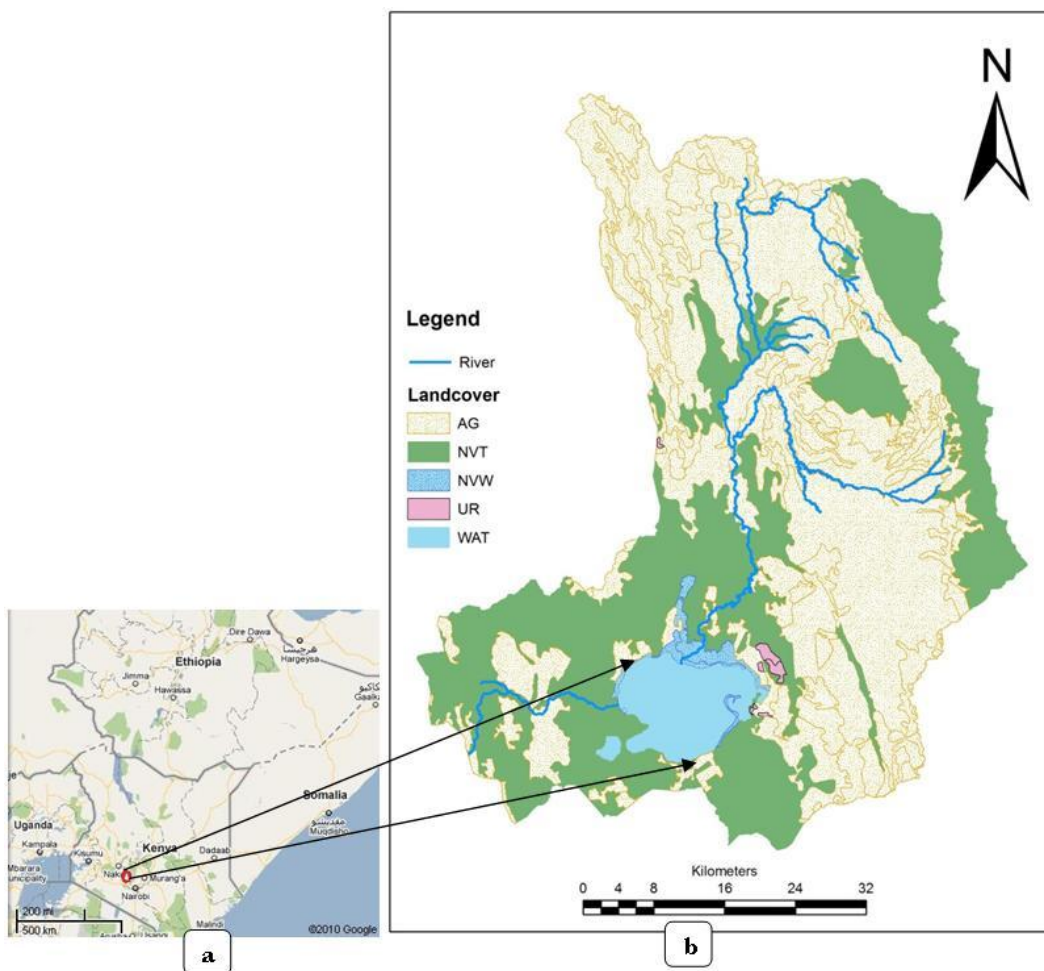
Figure 1: Layout of study area from a) Africa map and b) its overview as produced by FAO, 1999

3.1.2. Land use and climate

The major land use units of the catchment area are flowers growing and horticulture, dairy, forestry and papyrus swamp vegetation. The lake is an important freshwater resource for Kenya's foreign currency earning agriculture, tourism and water supply. Due to its international importance as a wetland it is Kenya's second Ramsar site though it supplies drinking water to Nakuru and irrigation water to the nationally important industries of horticulture and power generation (Becht and Harper, 2002). The climate of the basin is within the semi-arid belt of Kenya with the range of mean annual temperature of 25 degree Celsius on the shores of the lake to 16 degree Celsius on the Aberdares mountains and mean annual precipitation of 600 mm to 800 mm range while annual evaporation is approximately 1735 mm. Evaporation exceeds precipitation throughout the year except at peak rainfall. The rainfall trend is bimodal with a major peak in April to May and a minor one in September to October.

3.1.3. Drainage

The shallow body of water remains fresh due to inflow from river systems such as Gilgil (420 sq. km watershed) and Malewa and Karati (1750 sq. km watershed) and underground outflow through seepage. Gilgil and Malewa rivers flow into the lake from northern catchment while Karati River drains from northeast catchment though it is seasonal and does not reach the lake as surface water. Surface area of the lake Naivasha varies with an average range between 114 and 991 sq. km. This is due to the fact that the water level always experienced extensive water level fluctuations as a consequence of irregular rainfall patterns (Harper et al., 1990). The lake Naivasha has an average depth of 6 m with the deepest area being at Crescent Island (Crater Lake Game Sanctuary) at a maximum depth of 30 m though fluctuation in the water level of lake is a common phenomenon with low levels in the summer and high levels in the winter. Hydrological, ecological and geological backgrounds in the area are more described by Becht and Harper (2002), Harper et al. (1990), Harper (1992), Harper (2006), Harper et al. (1995) and Abiya (1996).

3.1.4. Socio Economic Importance

Horticultural farms use the lake water for irrigation. Fruits, vegetables and flowers are grown both for local and export market. Horticulture is of national importance as a source of foreign exchange and employment to some 30,000 people (Abiya, 1996; Gordon and Wang, 1994). Farms range in size from large companies with hundreds of hectares under intensive flower production to small farms growing vegetables for export. Dairy farms around the lake are well established and irrigated Lucerne farms have supported the industry since the late 1950s; however, intensive export oriented horticultural production has been developed only over the last 10 - 15 years and is still expanding. Besides its aforementioned values, the lake has the following socio economic importance:

- Geothermal power generation: a large volume of water is pumped from the lake and used in drilling new steam wells and in condensing existing steam;
- Domestic water supplies: this is obtained from the lake either directly or from wells or boreholes adjacent to the lake;
- Commercial fishing: the lake supports a thriving commercial fishery which started in 1959. The fish species (the largemouth bass, tilapine and crayfish) were introduced for exploitation. Crayfish is exploited both for export and local consumption;
- Tourism and recreation: the lake offers outstanding aesthetic scenery and recreational facilities such as boating, water-skiing, sport fishing, game viewing and bird watching;
- Ranching and game farming: the lake is utilized for game such as giraffe, buffalo, zebra, antelope, ostrich and waterbuck found within a number of ranches and game sanctuaries around the lake.

3.2. Analysis Methods

3.2.1. In situ Data Collection

Satellites do not measure absorption rather measure reflectance and radiation. Sensors can measure reflected (sun) radiation and emitted radiation. Its color is indicative of the amount of constituents for instance, CDOM and phytoplankton in the water. Interpretation of the color signature of satellite data is based on algorithms that relate remote sensing reflectance to CDOM concentration. It is theoretically possible to retrieve CDOM concentrations from optical measurements due to its spectral characteristics difference from the absorption spectra of chlorophyll and suspended matter. In ocean waters, absorption of CDOM is usually small compared to absorption by other constituents but some CDOM is likely to be present as the result of decaying phytoplankton especially at the end of a bloom. Unlike ocean waters, inland waters contain varying concentrations of dissolved organic compounds. One of these compounds' main sources is decayed terrestrial plant matter and thus, concentrations are high in lakes, rivers and coastal waters that are influenced by river runoff. These compounds are generally brown in color and it can color the water yellowish brown in sufficient concentrations. In such waters, CDOM can be the dominant absorber at the blue end of the spectrum. This color characteristic helps to connect the optical properties of the water body with its biogeochemical character.

Two data sources were used to boost the usefulness of satellite data for this research:

1. MERIS Satellite Imagery acquired on 20th, 23rd and 26th September 2010. In situ measurements were taken concurrently with MERIS overpass time to analyze the match-up of satellite retrieval of optical properties and water constituents. MERIS data along with Strategic sampling can provide spatial and temporal distribution of colored dissolved organic matter of the lake water body.
2. In situ measurements of apparent optical properties (AOPs) and inherent optical properties (IOPs) that were used for calibration of the algorithm and validation of satellite data. Sampling sites and frequency and timing of data collection were determined to investigate the spatial distribution of CDOM in the lake and its temporal differences in short terms.

Due to limited spatial resolution of satellite data, sampling points were set at minimum distance of 300 to 350 m apart from each other due to spatial resolution of MERIS (300 m x 300 m). Sampling sites were fixed in the regions in order to study the spatial scale of CDOM; however arbitrary points were taken for a single measurement study. The sites were marked using hand held Global Positioning System (GPS), Garmin 12XL. Collection of data on the whole lake area from fixed sampling sites and arbitrary points took four days on average, hereafter called Coverage. Three campaigns of coverage were made on the lake to collect data in order to analyze temporal differences in short terms:

*   Coverage 1 is from 17th September 2010 to 21th September 2010. Absorption coefficients of water constituents measured on 17th September 2010 were not used for statistical analysis due to laboratory measurement error;
*   Coverage 2 is from 23rd September 2010 to 28th September 2010. Measurement was not done on 22nd and 25th September 2010 due to cloud strips that biased the measurement of AOPs;
*   Coverage 3 is from 29th September 2010 to 3rd October 2010. Spectra and IOPs measurements from two sampling points were done by 29th September 2010 due to the high wind speed (> 8 m/sec). The wave on the lake water surface was more than 40 cm height that hindered the movement of the boat from site to site and stability of the boat was a problem to measure AOPs from a fixed point.
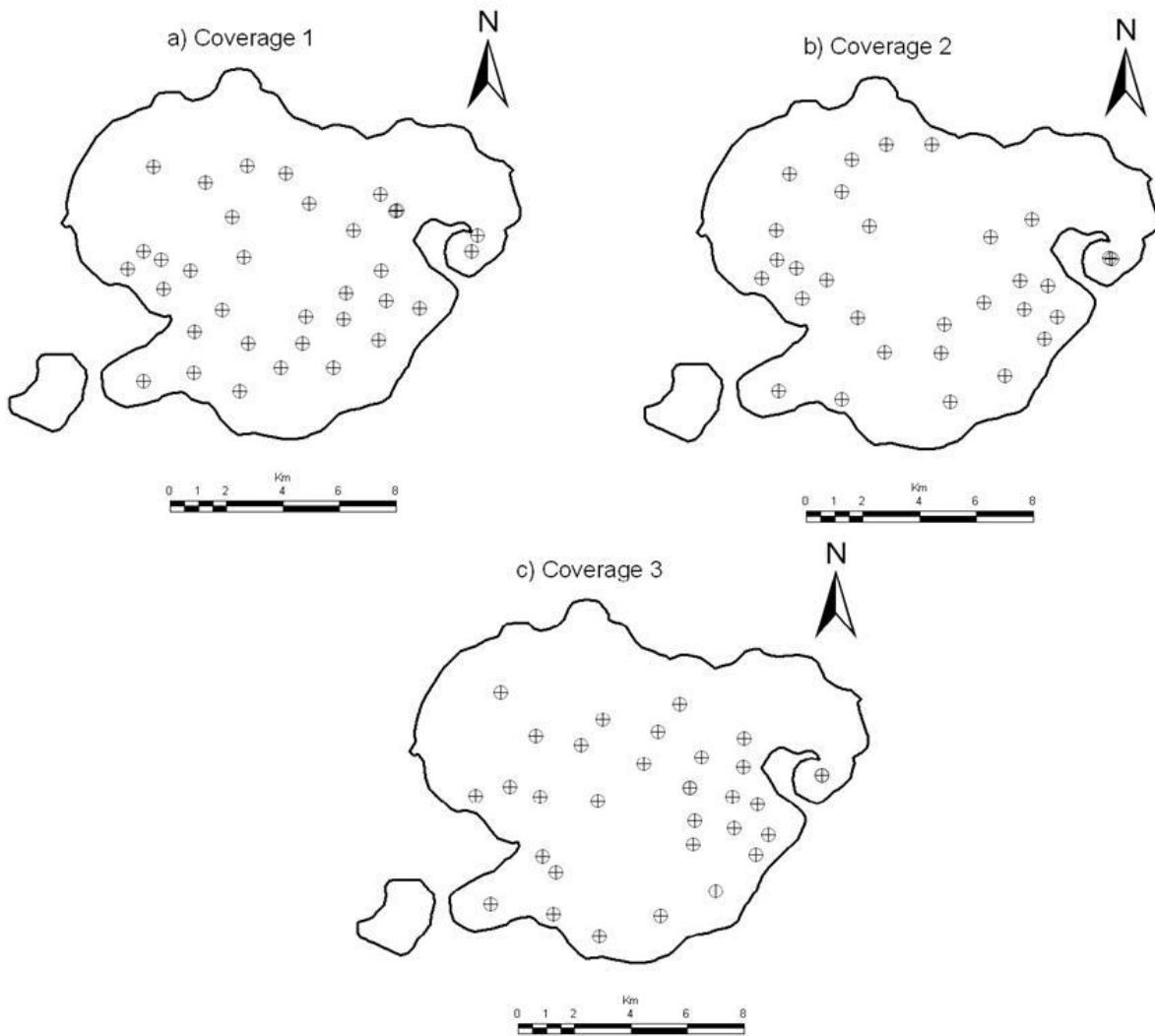
Figure 2: Three coverage where the water samples and spectra were collected simultaneously

The lake was categorized into six regions in order to investigate the spatial scale of CDOM of the lake water. Loads from rivers, discharges of domestic and industrial wastes, mar-culture activities and/or diffuse sources and minimal direct influence of both rivers and human activities were the main criteria considered for selection of sites for the assessment of water constituents' absorption in the regions:

- Crater lake Game Sanctuary: a site to the east of the lake where almost enclosed sub basin with minimal interaction from the main lake
- Gilgil inlet in the north: a turbid area where the principal rivers enter the lake
- Forest side: a site to the northwest of the lake with minimal direct influence of both rivers and human activities such as farming
- Hippo pool: a site to the southwest of the lake where huge number of hippopotamuses are found
- Flower industry in the south and southeast: a public entry point to the lake where washing and animal watering, farming activities in the riparian land and intensive horticultural industries take place
- Lake Centre regions to inspect diffuse sources

A total of 129 water samples for spectrophotometric analysis, and 169 optical measurements for calibration and validation of the algorithm were collected from 17th September 2010 to 3rd October 2010. With 125 sampling sites, both water samples and optical measurements were simultaneously achieved.

3.2.2.   Measurement of Apparent Optical Properties (AOPs)

Spectral remote sensing reflectance above water surface is the ratio of water leaving radiance to downwelling irradiance (Mobley, 1999).

$$R_{rs}(\lambda) = \frac{L_w(0^+, \lambda)}{E_s(0^+, \lambda)} \tag{1}$$

Where $R_{rs}(\lambda)$ is spectral remote sensing reflectance above water surface; λ is the wavelength; $L_w(0^+, \lambda)$ is the water leaving spectral radiance which is the radiance heading upward just above the water surface that originated from underwater light which is transmitted upward through the water surface; $E_s(0^+, \lambda)$ is the downwelling spectral plane irradiance incident onto the water surface.

Water leaving reflectance relates physical and biological properties of the sea water. The $R_{rs}(\lambda)$ spectrum contains subsurface information of water constituents and bottom properties for optically shallow water. Using a handheld spectroradiometer, a series (~ 3 to 7 scans) of upwelling radiance just above the water surface and the downwelling irradiance ($E_s(0^+, \lambda)$) were directly measured by the instruments, TriOS Optical Sensors, for each selected sites. All optical measurements were undertaken following the NASA protocols described in Mueller et al. (2002). The measured upwelling radiance just above the water surface is a sum of photons emerged from subsurface scattering (the desired signal) and surface reflected sky and solar light (noise). In situ measurements of downwelling irradiance and upwelling radiance just above the water and from gray Spectralon were carried out using handheld Spectrum Acquisition Module (RAMSES radiometer) sensors over the lake Naivasha, which are designed for combining precision hyperspectral light measurement with a maximum of flexibility.

The upwelling radiance just above the water surface was collected using RAMSES-ARC (Hyperspectral UV-VIS Radiance Sensor) device placed just above the water surface and connected to the Data Logger, Data Storage with Power Pack (DSP). Another Spectrum Acquisition Module (SAM) sensor connected to DSP was RAMSES-ACC-VIS (Hyperspectral UV-VIS Irradiance Sensor) to collect downwelling irradiance ($E_s(0^+, \lambda)$). DSP supplies them with power and triggers measurements simultaneously. The operational range of both RAMSES radiometer family sensors is from the near ultraviolet to the near infrared (320 nm - 950 nm) wavelengths with average increments of 3.33 nm. The measurement data was stored in its internal memory card with timestamp.
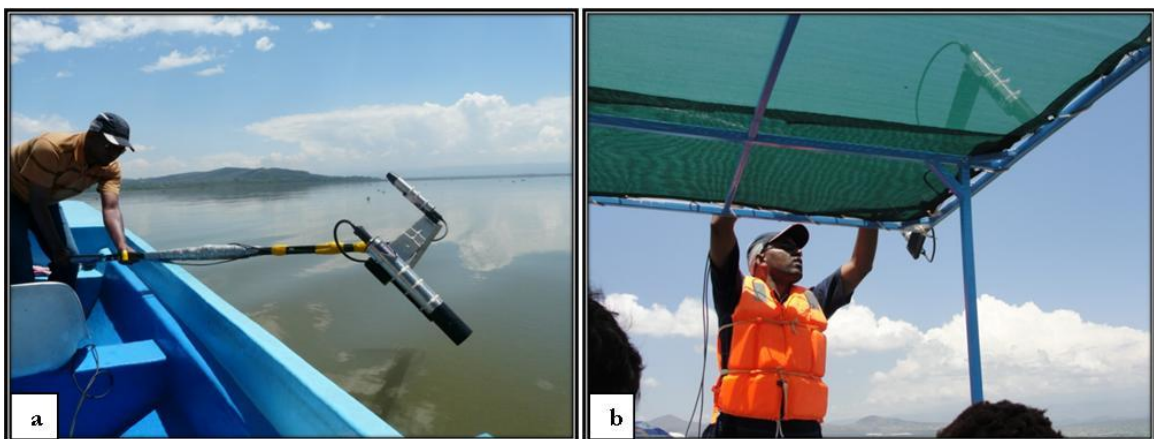
Figure 3: Optical measurements just above the water a) upwelling radiance b) downwelling irradiance

Although the downwelling irradiance ($E_s(0^+, \lambda)$) could be measured directly with available instrument, such a measurement was not possible for water leaving radiance. This is because a radiometer pointing toward the water surface measures the sum of the water leaving radiance and any incident sky radiance (Mobley, 1999) that has been reflected by the lake water surface.

$$R_{rs}(\lambda) = \frac{L_u(0^+, \lambda) - F.L_{sky}(\lambda)}{E_s(0^+, \lambda)} \qquad (2)$$

Where $E_u(0^+, \lambda)$ is upwelling radiance just above the water surface; F is surface Fresnel reflectance (air-water interface specular reflection coefficient for radiance); $L_{sky}(\lambda)$ is sky radiance.

Sky radiance in any downward direction can in principle be reflected by the wavy surface into the detector. The lake water surface was calm with wind speed less than 2m/sec during in situ data acquisition so that water surface reflectance ($F.L_{sky}(\lambda)$) was negligible and hence, upwelling water radiance and downwelling irradiance were used to derive remote sensing reflectance using the relation below:

$$R_{rs}(\lambda) = \frac{L_u(0^+, \lambda)}{E_s(0^+, \lambda)} \qquad (3)$$

Remote sensing reflectance was derived from measured radiance reflected from gray Spectralon after RAMSES-ACC-VIS Sensor was failed to transfer data to the DSP. Downwelling irradiance was derived by measuring the radiance reflected from a standard diffuse reflector (Spectralon®) called Lambertian reflector (gray Spectralon). For each of the collected scans, hyperspectral remote sensing reflectance was derived through the following relation (Lee et al., 2007):

$$E_s(0^+, \lambda) = \frac{L_R(\lambda).\pi}{R_R} \qquad (4)$$

$$R_{rs}(\lambda) = \frac{(L_u(0^+, \lambda) - F.L_{sky}(\lambda)).R_R}{\pi.L_R(\lambda)} \qquad (5)$$

Where $L_R(\lambda)$ is radgraye reflected from grey Spectralon; R_R is the reflectance of the diffuse reflector which was adopted as 99% (Doxaran et al., 2004). Considering the negligible water surface reflectance due to the calmness of the lake water surface, equation (4) and equation (5) were combined and simplified as:

$$R_{rs}(\lambda) = \frac{(L_u(0^+, \lambda)).(0.99)}{\pi.L_R(\lambda)} \qquad (6)$$

3.2.3. Measurement of Inherent Optical Properties (IOPs)

Water was collected for spectrophotometric analyses. The water samples were taken just below the water surface using one litre size polyethylene bottles. Polyethylene bottles were temporally stored in the boat by wrapping the bottles with aluminium foil until arriving in the laboratory, where the samples were immediately transferred to a refrigerator and then processed. Samples were run fresh as recommended by Tilstone et al.(2002). In order to prevent bacterial growth and degradation of water constituents that in turn reduces analytical errors in MERIS data validation.

Samples were collected between 9:00 a.m. and 12:00 a.m. local time in the morning and analyzed between 12:30 a.m. and 7:00 p.m. local time in the afternoon in the laboratory established by Prof. D.M. Harper which is located about 1 to 1.5 km farther distance from the Yacht beach. Spectral absorptions by total and CDOM were measured in the laboratory using a standard laboratory bench cuvette system, DR/2000

Spectrophotometer with 10 mm quartz cell at specific wavelengths such as 400 nm, 412 nm, 440 nm, 443 nm, 490 nm, 555 nm and 750 nm. The total absorption coefficients were determined by the cuvette from water samples before any filtration process. Water samples for CDOM absorption underwent a two step filtration processes. The first filtration was through GF/F, nominal pore size 0.7µm. This was pre-filtration for the next filtration process. The advantage of the first filtration was to prevent clogging of 0.2 µm size filters and ease passage of CDOM through 0.2 µm filters for analysis.

Subsamples then were filtered through 0.2 µm Anotop Syringe filters and stored in 100 mL distilled water-cleaned amber glass bottles for determination of absorption coefficients of CDOM. The 0.2 µm filtration step was very labor intensive. A fresh filter was used for each sample. After filtration over 0.2 µm filters, the filtrate only contained dissolved matter with negligible scattering in the visible light wavelength region. The filtrate was kept at room temperature and the absorption of the filtrate was measured in the cuvette. A background correction was applied by subtracting the absorbance value at 750 nm from all the spectral values (Babin et al., 2003b).

The absorption coefficients of samples were obtained by measuring the signal from the samples against the signal of a reference solution, distilled water that was used as the reference blank ($a_w(\lambda) = 0$) for all measurements and subtracted from the sample spectra. DR/2000 Spectrophotometer measures absorbance (A). The absorbance of a sample is expressed as the ratio of these signals, corrected for the background signal. The spectral absorption coefficients of total and CDOM were calculated from measured absorbance using the equation derived from the Beer-Lambert law (Green and Blough, 1994) by applying baseline correction for scattering effects by subtracting the absorption value of total and CDOM at 750 nm from the whole total and CDOM spectrum respectively. The absorption coefficients which are dependent on the path length were calculated as follows:

$$a_t(\lambda) = \frac{\ln(10).(A_\lambda - A_{750})}{l} \tag{7}$$

$$a_{CDOM}(\lambda) = \frac{\ln(10).(A_\lambda - A_{750})}{l} \tag{8}$$

Where $a_{CDOM}(\lambda)$ is the absorption coefficient of CDOM [m^{-1}] at wavelength (λ); $a_t(\lambda)$ is the absorption coefficient of total [m^{-1}] at wavelength (λ); A_λ is the respective measured absorbance of light at the same wavelength; A_{750} is the respective absorbance of light at a reference wavelength (750 nm); l is the light path length of the cuvette [m]; $a_w(\lambda)$ is absorption coefficient of water.

The absorption coefficients of particles were derived from measured absorption coefficients of total and CDOM as follows:

$$a_P(\lambda) = a_t(\lambda) - a_{CDOM}(\lambda) \tag{9}$$

Where $a_P(\lambda)$ is absorption coefficients of particles [m^{-1}] that comprises absorption coefficients of non algal particles ($a_{NAP}(\lambda)$) and phytoplankton ($a_\phi(\lambda)$).

Terrestrial and marine derived CDOM have absorption spectra that decrease exponentially toward longer wavelengths. The reference wavelength of 443nm was chosen (Be´langer et al., 2008) because it corresponds approximately to the midpoint of the blue-green chlorophyll absorption. Because the CDOM absorption has an exponentially declining shape without distinctive peaks, any wavelength can be used as a reference although it is preferable to use a wavelength in the blue-green region where the CDOM absorption is the highest.

This exponential shape is thought to be the theoretical form of CDOM absorption and measured CDOM absorption spectra which are usually corrected by fitting an exponential function:

$$a_{CDOM}(\lambda) = a_{CDOM}(\lambda_0).\exp^{(S.(\lambda_0 - \lambda))} \tag{10}$$

Where λ_0 is reference wavelength (443nm); $a_{CDOM}(\lambda_0)$ is absorption coefficient of CDOM at reference wavelength and S is the spectral slope of the exponential function.

3.2.4. CDOM Model

Concentrations of optically active constituents in the upper layer of the observed water body can be determined using empirical algorithms based on statistical relationships. The advantages of empirically-derived algorithms are that they are simple, easy to derive even from a limited number of measurements (provided they cover the desired range of measurements), and easy to implement and test. They have a short computing time due to their mathematical simplicity, and they yield stable results, provided the scope of the algorithm is not violated. By their very nature, empirical algorithms for Case 2 waters are always regional in scope (Corbett et al., 2007). In empirical methods, statistical relations are determined between parts of the spectrum (combination of band ratios) by means of regression analysis to a set of in-situ measured concentrations.

In global ocean color studies, empirical algorithms are quite commonplace and give good results because they are based on large datasets (O'Reilly et al., 1998). Inland waters have a much larger diversity and ranges of concentrations, which causes empirical algorithms to be site specific. The $a_{CDOM}/a_t(412)$ was regressed against combinations and ratios of $R_{rs}(\lambda)$ selected according to the following rationales: in case 2 waters, reflectance at 412 nm is the most affected by CDOM absorption, reflectance at 490 nm is the most affected by phytoplankton absorption, variations in reflectance at 555 nm is mostly driven by light scattering by suspended particles, and a major distinctive property of CDOM is that it does not contribute to particle scattering. These considerations led to propose the empirical algorithm for the retrieval of $a_{CDOM}/a_t(412)$. This empirical algorithm which is used in optically complex waters was developed by Be´langer et al. (2008) and Gallegos and Neale (2002).

$$\frac{a_{CDOM}}{a_t}(412) = \alpha + \beta.\log10\frac{R_{rs}(412)}{R_{rs}(555)} + \chi.\log10\frac{R_{rs}(490)}{R_{rs}(555)} + \delta.\log10(R_{rs}(555)) \tag{11}$$

Where α, β, χ and δ are empirical coefficients.

In the open ocean, there is significant absorption by pure water itself; however, in optically complex water absorption by pure water is negligible compared to non-water absorption coefficients over the 300 nm to 500 nm range (Be´langer et al., 2008). For a particular value of the ratio at 412 nm ($a_{CDOM}/a_t(412)$), $a_{CDOM}/a_t(\lambda)$ can be calculated if the spectral slope of CDOM spectrum and the spectral shape of the particulate absorptions from field observations in the lake are known. Therefore, the spectral extrapolation of $a_{CDOM}/a_t(412)$ can be achieved with known spectral slope of CDOM and particle absorption at wavelength, λ normalized to particle absorption at 412 nm.

$$\frac{a_{CDOM}}{a_t}(\lambda) = \frac{f.\exp^{(S(412-\lambda))}}{f.\exp^{(S(412-\lambda))} + (1-f).a_P^N(\lambda)} \tag{12}$$

Where $a_P^N(\lambda)$ is $a_P(\lambda)$ spectrum normalized to $a_P(412)$ ($a_P^N(\lambda) = a_P(\lambda)/a_P(412)$); $f = a_{CDOM}/a_t(412)$; $a_{CDOM}(\lambda)$ can be expressed using equation (10); S is spectral slope of CDOM ($0.014nm^{-1}$) in the lake that was derived using measured absorption coefficients of CDOM of the lake water from 93 samples at specific wavelengths:400 nm, 412 nm, 440 nm, 443 nm, 490 nm and 555 nm with 443 nm as reference wavelength.

3.2.5. Atmospheric Correction

Empirical algorithms can operate on raw image data which eliminates the need for atmospheric correction of the image. It is recommended to apply atmospheric correction to the data and use band ratios if possible when looking at multitemporal observations in the same area (Laanen, 2007). Remote sensing of

ocean color initially focused primarily on the retrieval of the concentration of chlorophyll *a* in the global oceans. Subsequent studies, however, have also emphasized the importance of understanding and retrieving via remote sensing of ocean color, inherent optical properties (IOPs), namely, the absorption and scattering characteristics of water and its constituents (the dissolved and suspended materials). Variations in IOPs are clear indications of changes in water constituents.

The information retrieved from ocean color remote sensing can contribute to our understanding of the planetary carbon cycle and climate research as well as other biological and biogeochemical processes in the oceans, and has many other applications including management of marine resources (Corbett et al., 2007). The MERIS product for CDOM concentration retrieval in lake Naivasha helps environmental managers to assess its CDOM status and to set up or modify the framework of monitoring protocols of the lake Naivasha. MERIS is a wide field of view ocean color sensor aboard the European Space Agency's ENVISAT satellite. MERIS measures visible and near infrared light that are scattered by the earth and thus, it is used for monitoring of land, atmosphere and ice although primarily designed for ocean color observation. It has high spectral and radiometric resolutions which meet the requirement for global ocean observation. MERIS has spectral bands in the red and near-infrared region combined with high resolution observation which is a great advantage of coastal and inland water monitoring. It has 15 spectral bands in the 390 nm – 1040 nm range with spectral resolution of 10 nm.

Conventional ocean color bands (412.5 nm, 442.5 nm, 490 nm, 510 nm, 560 nm and 620 nm) are suitable for monitoring chlorophyll *a*; colored dissolved organic matter and suspended particles. It operates in Full Resolution (FR) of 300 m and Reduced Resolution (RR) of 1200 m modes of ground resolution. The RR mode is suitable for open ocean observation and operated in a routine manner. On the contrary, the FR mode is useful for coastal and inland water observations and operated on request.

MERIS Level 1b of Full Resolution (FR) satellite image data that were acquired from the ESA's ENVISAT was used in this study. Among the satellite data available, there were three MERIS data, a full matchup in time with in situ measurements, 20th, 23rd and 26th September 2010. These data were used to analyze the matchup of satellite retrieval of optical properties and water constituent with in situ observations. The processes of scattering and absorption by dissolved and suspended materials in the water body affect the spectrum and radiance distribution (light field) of the light emerging from the lake water the so called water leaving radiance. If the atmosphere and surface effects can be removed successfully, inversions of the water leaving radiance are the absorption and scattering characteristics of the dissolved and suspended materials and hence, atmospheric correction was carried out following the method adopted by Gordon and Wang (1994).

$$R_{rs(t)}^{(\lambda)} = T_g^{(\lambda)}.(T_v^{(\lambda)}.R_{rs(sfc)}^{(\lambda)} + R_{rs(Path)}^{(\lambda)} + T_v^{(\lambda)}.R_{rs(w)}^{(\lambda)})$$

(13)

Where $R_{rs(t)}^{(\lambda)}$ is recorded reflectance at sensor level; $T_g^{(\lambda)}$ is gaseous transmittance; $T_v^{(\lambda)}$ is diffuse transmittance; $R_{rs(sfc)}^{(\lambda)}$ is sea-surface reflectance; $R_{rs(Path)}^{(\lambda)}$ is atmospheric path reflectance that combines scattering of aerosol ($R_{rs(a)}^{(\lambda)}$) and air molecules ($R_{rs(r)}^{(\lambda)}$); $R_{rs(w)}^{(\lambda)}$ is water leaving reflectance. The lake water surface reflectance is neglected as discussed under section 3.2.2. Only few gases produces observable absorption features in the spectral regions between 400nm and 1000nm (McKnight and Aiken, 1998) and hence, gaseous transmittance is assumed to be unity. Therefore, equation (13) is reduced to:

$$R_{rs(t)}^{(\lambda)} = R_{rs(Path)}^{(\lambda)} + T_v^{(\lambda)}.R_{rs(w)}^{(\lambda)}$$

(14)

Where $T_v^{(\lambda)}$ and $R_{rs(Path)}^{(\lambda)}$ were derived from recorded reflectance at sensor level (MERIS), $R_{rs(t)}^{(\lambda)}$ and measured water leaving reflectance, $R_{rs(w)}^{(\lambda)}$. The values of $T_v^{(\lambda)}$ and $R_{rs(Path)}^{(\lambda)}$ can be referred from Table 7.

4.   RESULTS AND DISCUSSIONS

4.1.   Field Spectra

The downwelling irradiance ($E_s(0^+, \lambda)$) and upwelling radiance ($L_u(0^+, \lambda)$) obtained from different scans of a site were averaged for different sites, rejecting outliers which were more than 5% in the blue (Be´langer et al., 2008) in order to reduce the random variations as associated with the measurements before using their value to derive $R_{rs}(\lambda)$.
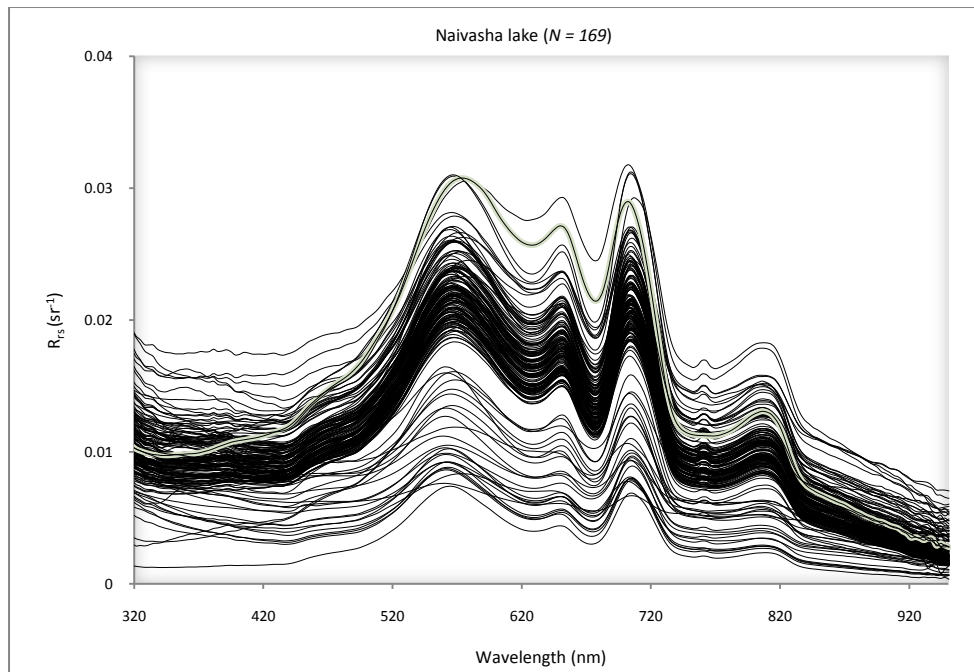
Figure 4: Total envelope of spectra of lake Naivasha for 169 sampling points collected from 17 September 2010 to 3 October 2010

For the assessment of absorptions water constituents, the lake was categorized into six regions. Optical measurements were collected from arbitrary and fixed sampling points in the regions in an attempt to observe the spatial spectra of the lake water. The spectra of lake Naivasha in the six categorized regions are shown in Figure 5. The observations are at different days from 17th September to 3rd October 2010.
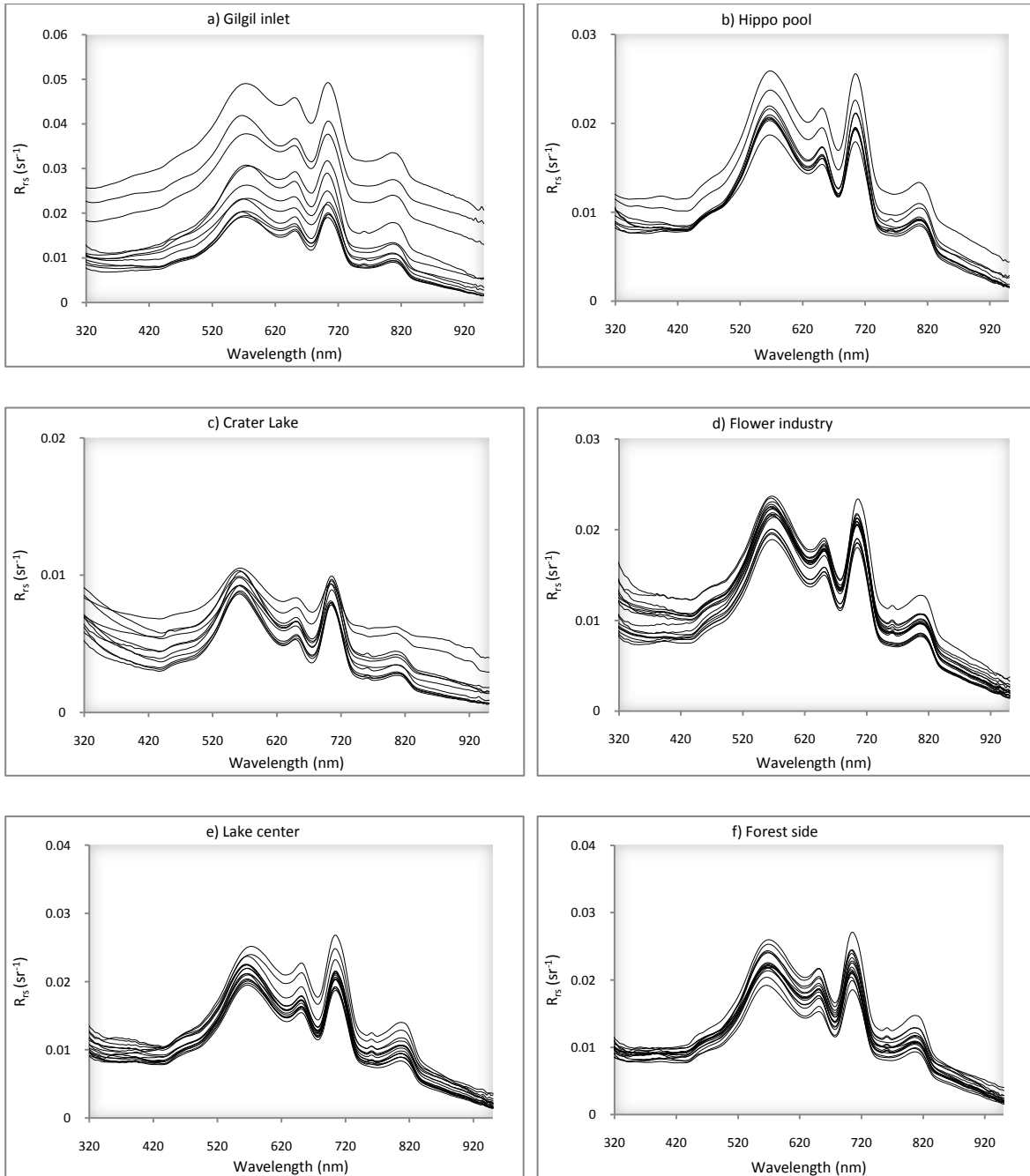
Figure 5: Spectra of lake Naivasha for different regions observed at different days (26/09-3/10/2010)

The average spectra of the lake and its regions are given in Figure 6. From this figure one can clearly observe that correlation between reflectance and turbidity. The reflectance at Gilgil inlet is apparently high. This is associated with increases in wet season flow that brings considerable quantities of terrestrial plant materials to the lake that increase turbidity and hence, remote sensing reflectance increases as the turbidity increases. On the other hand, reflectance in Crater lake is low. This lower value of remote sensing reflectance is due to the absence of direct influence of river runoff that improves turbidity.
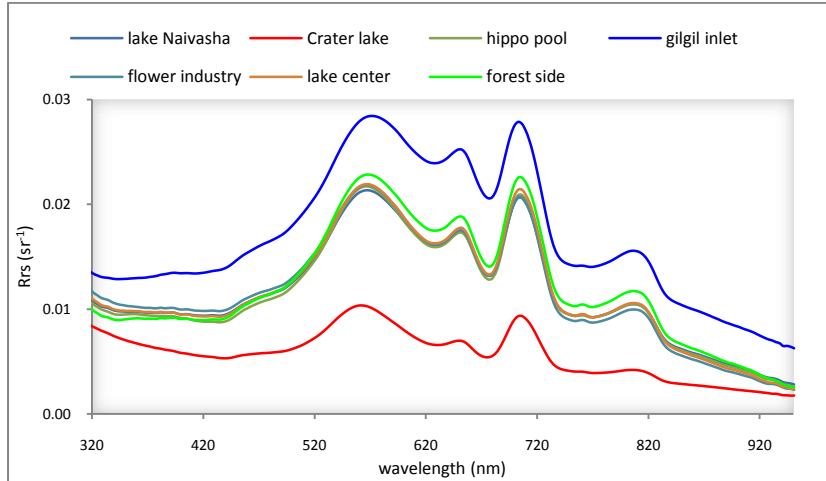
Figure 6: Average spectra of the lake and its regions observed at different days (26/09 – 3/10/2010)

4.2. Laboratory Results (IOPs)

The number and location of sampling points were decided to evaluate spatial and temporal (in short terms) characteristics of the lake water taking into account the data requirements, the cost effective sampling plan and time allocated for data collection.

Table 1: Average absorptions of constituents, a_{CDOM}/a_t at 412 nm and slope of CDOM in the lake

Lake regions	[1]N	Absorption coefficients			a_{CDOM}/a_t	Spectral Slope (nm^{-1})
		$a_t(m^{-1})$	$a_{CDOM}(m^{-1})$	$a_P(m^{-1})$		
Gilgil inlet	3	23.95 ± 8.98	3.99 ± 0.87	19.96 ± 9.85	0.19 ± 0.09	
Hippo pool	11	17.44 ± 2.58	4.46 ± 0.42	12.98 ± 2.34	0.26 ± 0.03	
Crater Lake	7	7.83 ± 1.19	4.31 ± 0.51	3.52 ± 1.01	0.56 ± 0.08	
Flower industry	14	14.94 ± 1.42	3.95 ± 0.39	10.99 ± 1.51	0.27 ± 0.04	
Lake centre	7	17.57 ± 3.13	4.15 ± 0.35	13.42 ± 3.31	0.24 ± 0.05	
Forest side	11	21.73 ± 4.44	4.19 ± 0.70	17.54 ± 4.67	0.20 ± 0.06	
Lake Naivasha	93	18.42 ± 5.44	4.06 ± 0.63	14.36 ± 5.51	0.24 ± 0.11	0.014 ± 0.004

[1]*N is number of sampling pointes where samples and spectra were collected concurrently*

The value of a_{CDOM}/a_t at 412 nm for lake Naivasha varies between 0.09 (associated with main lake) and 0.67 (associated with Crater lake) with an average value of 0.24 ± 0.11. The average values of a_{CDOM}/a_t at 412 nm were found to be 0.22 ± 0.05 and 0.56 ± 0.08 in main lake and Crater lake respectively.

Table 2: Average absorption coefficients of water constituents in Main lake and Crater lake

Parameters	Crater lake ($N=7$)			Main lake ($N=86$)			Whole lake ($N=93$)		
	Min	Max	Avg.	Min	Max	Avg.	Min	Max	Avg.
$a_t(m^{-1})$	6.68	9.90	7.83	13.59	38.23	19.28	6.68	38.23	18.42
$a_{CDOM}(m^{-1})$	3.68	5.07	4.31	2.30	5.53	4.04	2.30	5.53	4.06
$a_P(m^{-1})$	2.30	4.84	3.52	9.44	34.31	15.25	2.30	34.31	14.36
a_{CDOM}/a_t	0.47	0.67	0.56	0.09	0.31	0.22	0.09	0.67	0.24
$Slope(nm^{-1})$					0.014				

Less cloud coverage was considered when determining frequency and timing of data collection. Full coverage of the whole lake area was made three times so that data were collected from whole lake per coverage to analyse temporal differences. Temporal differences can be observed from Table 3 by focusing the monitoring time in short terms under less cloud coverage. Temporal variability of absorptions of particles is apparently high compared to absorptions of CDOM which can be an indication tool for presence of temporal variability of absorption coefficients of suspended particles. This is because of inflowing from three perennial river systems, and smaller and seasonal streams into the lake that influences the concentration and distribution of nutrients and biochemical elements.

Table 3: Average values of measured parameters of constituents in the lake as of coverage

Parameters	Coverage								
	$18/09/10 - 21/09/2010$			$23/09/10 - 28/09/2010$			$29/09/10 - 03/10/2010$		
	$N = 34$			$N = 29$			$N = 30$		
	Max	Min	Avg.	Max	Min	Avg.	Max	Min	Avg.
$a_t(m^{-1})$	34.31	8.98	21.27 ± 4.32	38.23	6.91	18.98 ± 6.48	17.50	6.68	14.65 ± 2.76
$a_{CDOM}(m^{-1})$	5.53	2.99	4.33 ± 0.63	5.07	2.30	3.80 ± 0.66	5.06	2.76	4.00 ± 0.49
$a_P(m^{-1})$	31.32	4.61	16.94 ± 4.60	34.31	2.30	15.18 ± 6.56	13.82	2.53	10.65 ± 2.82
a_{CDOM}/a_t	0.51	0.09	0.22 ± 0.08	0.67	0.10	0.23 ± 0.11	0.65	0.18	0.29 ± 0.11
$Slope(nm^{-1})$			0.012 ± 0.004			0.015 ± 0.003			0.016 ± 0.003

Variability of absorptions of particles is high in main lake compared to the Crater lake as can be seen from pictures collected (Figure 7 and Figure 8) during field campaign.

Figure 7: Pictures of clear water collected from the Crater lake

Figure 8: Pictures of fluctuation of water color due to suspended particles in the main lake collected during field campaign

The measured absorptions of total and CDOM, and spectra used as input dataset for statistical analysis were from 93 sampling sites. Measurements from 32 sites were discarded because of their errors in the measurements of the spectra, concentrations of CDOM or/and concentrations total. Sources of errors were instrument accuracy, movement of the boat while taking optical measurements, cloud spots, aquatic suspended vegetations, measurement errors, sun glint, water surface roughness, shallow depth and foam. Figure 9(a) and (b) presents absorption spectra of CDOM that decrease exponentially toward longer wavelengths for all samples collected from 93 sampling points and average of it respectively.
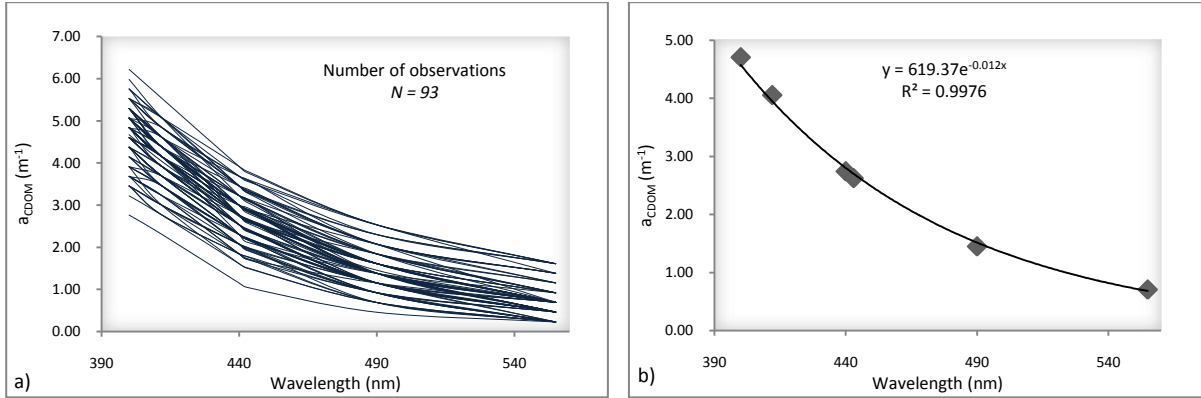
Figure 9: a) Absorption coefficients of CDOM in lake Naivasha from all sampling points; b) the averaged values of CDOM absorption (diamonds) and the fitting exponential function (line).

4.3.   Retrieval of a_{CDOM}/a_t Ratio from Remote Sensing Reflectance

Optical properties of CDOM play an important role in quantitative water color remote sensing retrieval. Empirical coefficients were derived applying the relations developed (Equation (11)) by multiple regression which was conducted using measured $a_{CDOM}/a_t(412)$ ratio and $R_{rs}(\lambda)$ at 412 nm, 490 nm and 555 nm. Table 4 provides the multiple regression results for the coefficients of equation (11) whose p-values are significantly less than 5%, and the determination coefficient (R^2). The empirical coefficients were derived using whole dataset (absorptions of total and CDOM, and spectra) obtained on the lake using multiple regressions.

Table 4: Empirical coefficients of equation (11) by multiple regression

Name	N	α	β	χ	δ	R^2
lake Naivasha	93	-0.993	1.202	-1.212	-0.804	0.81

Comparison between the retrieved and measured $a_{CDOM}/a_t(412)$ values is shown Figure 10. Retrieved $a_{CDOM}/a_t(412)$ ratio was derived from spectra collected by handheld spectroradiometer using equation (11) with coefficients tabulated in Table 4.
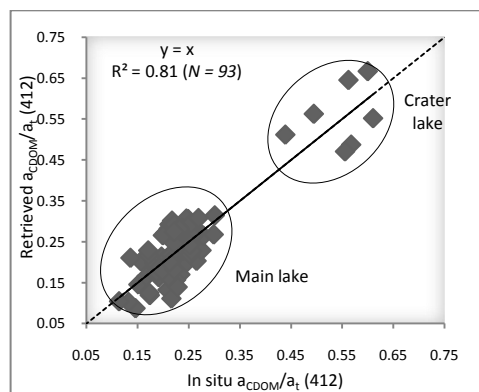
Figure 10: Comparison plot of retrieved and in situ measured a_{CDOM}/a_t at 412 nm. Dashed lines are the 1:1 reference lines, and full lines are the linear regression between the data points on x and y axes.

The isolated scatter points at the right end of the line in Figure 10 are due to the high values of a_{CDOM}/a_t at 412 nm in Crater lake compared to the main lake; this is due to less absorption coefficients of suspended particles in Crater lake (Table 1).

The comparison between retrieved and measured values was performed using Type II regression. The root mean squared error between measured and retrieved values was computed as:

$$RMSE = \sqrt{\frac{\sum_{i=1}^{n}\left([a_{CDOM}/a_t]_i^{measured} - [(a_{CDOM}/a_t)]_i^{retrieved}\right)^2}{n}} \qquad (15)$$

Where $(a_{CDOM}/a_t)^{measured}$ and $(a_{CDOM}/a_t)^{retrieved}$ are the measured and retrieved values of a_{CDOM}/a_t at 412 nm respectively. Table 5 shows the results of the comparison.

Table 5: Results of regression between retrieved and measured a_{CDOM}/a_t at 412 nm

Name	N	$Slope$	$Intecept$	R^2	$RMSE$
Lake Naivasha	93	1	0.00	0.81	0.05

4.4. Application to MERIS Imagery

The objective in this section is to estimate a_{CDOM}/a_t at 412 nm from MERIS imageries. The empirical algorithm (Equation (11)) using the empirically derived coefficients (Table 4) was applied to Full Resolution MERIS imageries of the lake Naivasha acquired on 20nd, 23rd, and 26th September 2010. The images were processed by the matchup of satellite retrieval of optical properties and water constituents with concurrent in situ observations using equations (14). Atmospheric path reflectance and diffuse transmittance were generated by optimization using solver plug-in embedded in Microsoft excel 2007®. Comparisons between the retrieved and measured a_{CDOM}/a_t at 412 nm values are shown Figure 11.
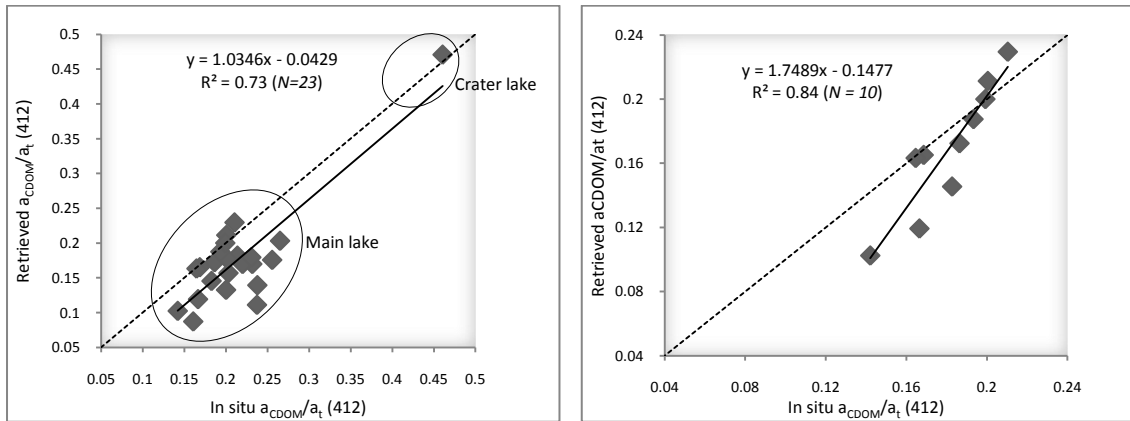
Figure 11: Comparison between retrieved (from MERIS) and measured a_{CDOM}/a_t at 412nm a) before cloud masking b) after cloud masking. Dashed lines are the 1:1 reference lines, and full lines are the linear regression between the data points on x and y axes.

The estimation of $a_{CDOM}/a_t(412)$ from satellite imageries along with strategic sampling and measuring the absorptions of total will lead to the calculation of values of absorptions of CDOM in the lake Naivasha.

Retrieved $a_{CDOM}/a_t(412)$ was retrieved using remote sensing reflectance derived from MERIS imageries that were corrected with coefficients tabulated in Table 7. Comparison presented in Figure 11(b) was

achieved with extra masking of cloudy data because of the image acquired on 26 Sept 2010 was blurred0 due to cloud spots. Table 5 shows the results of the comparison.

Table 6: Results of regression between retrieved (from MERIS) and measured a_{CDOM}/a_t at 412 nm

Name	N	Slope	Intecept	R^2	RMSE
Before cloud masking					
Lake Naivasha	23	1.03	0.04	0.73	0.05
After cloud masking					
Lake Naivasha	10	1.75	0.15	0.84	0.03

Moreover, the values of the spectra collected from in situ seem exaggerated in the main lake; this is because of the reflectance of floating-leaved plants, *Nymphaea caerulea* and suspended particles though these plants and particles are absent in Crater lake (Figure 7 and Figure 8). A point at the right end of Figure 11(a) is seen back in in-situ and MERIS that was taken from Crater lake.

Table 7: Atmospheric path reflectance and diffuse transmittance generated for atmospheric correction

MERIS wavelength	20-Sep-10			23-Sep-10			26-Sep-10		
	RMSE	$R_{rs(Path)}^{(\lambda)}$	$T_v^{(\lambda)}$	RMSE	$R_{rs(Path)}^{(\lambda)}$	$T_v^{(\lambda)}$	RMSE	$R_{rs(Path)}^{(\lambda)}$	$T_v^{(\lambda)}$
412.6910	0.0058	0.1181	1	0.0028	0.1239	0.4568	0.0093	0.1291	0.4231
442.5590	0.0059	0.0894	1	0.0030	0.0957	0.5435	0.0093	0.1033	0.5731
489.8820	0.0061	0.0573	1	0.0030	0.0684	0.6086	0.0091	0.0776	0.6748
509.8190	0.0064	0.0455	1	0.0035	0.0581	0.6665	0.0090	0.0722	0.6228
559.6940	0.0080	0.0201	1	0.0049	0.0405	0.7446	0.0094	0.0647	0.5976
619.6010	0.0093	0.0132	1	0.0046	0.0275	0.7939	0.0089	0.0479	0.7005
664.5731	0.0096	0.0121	1	0.0044	0.0224	0.8626	0.0091	0.0387	0.8652
680.8210	0.0097	0.0118	1	0.0043	0.0209	0.8628	0.0089	0.0320	1
708.3290	0.0121	0.0058	1	0.0060	0.0164	0.9421	0.0094	0.0474	0.7155
753.3710	0.0200	0.0169	1	0.0083	0.0181	1	0.0091	0.0345	1
761.5081	0.0146	0.0175	1	0.0062	0.0105	1	0.0079	0.0053	1
778.4091	0.0207	0.0160	1	0.0087	0.0172	1	0.0089	0.0336	1
864.8760	0.0229	0.0167	1	0.0083	0.0152	1	0.0087	0.0327	1
884.9444	0.0234	0.0163	1	0.0084	0.0144	1	0.0087	0.0314	1
900.0001	0.0186	0.0066	1	0.0065	0.0088	1	0.0069	0.0195	1

Correlation shown under Figure 11 is produced from atmospherically corrected MERIS image for points where in situ data were collected. Therefore, in order to apply on the whole lake (pixel bases), generation of $R_{rs}(\lambda)$ from MERIS L1 data was extended to all pixels using BEAM software which is mainly dedicated to data of imaging ENVISAT sensors. The $a_{CDOM}/a_t(412)$, calculated using equation (11) with coefficients (Table 4) shows coherent patterns over the lake.
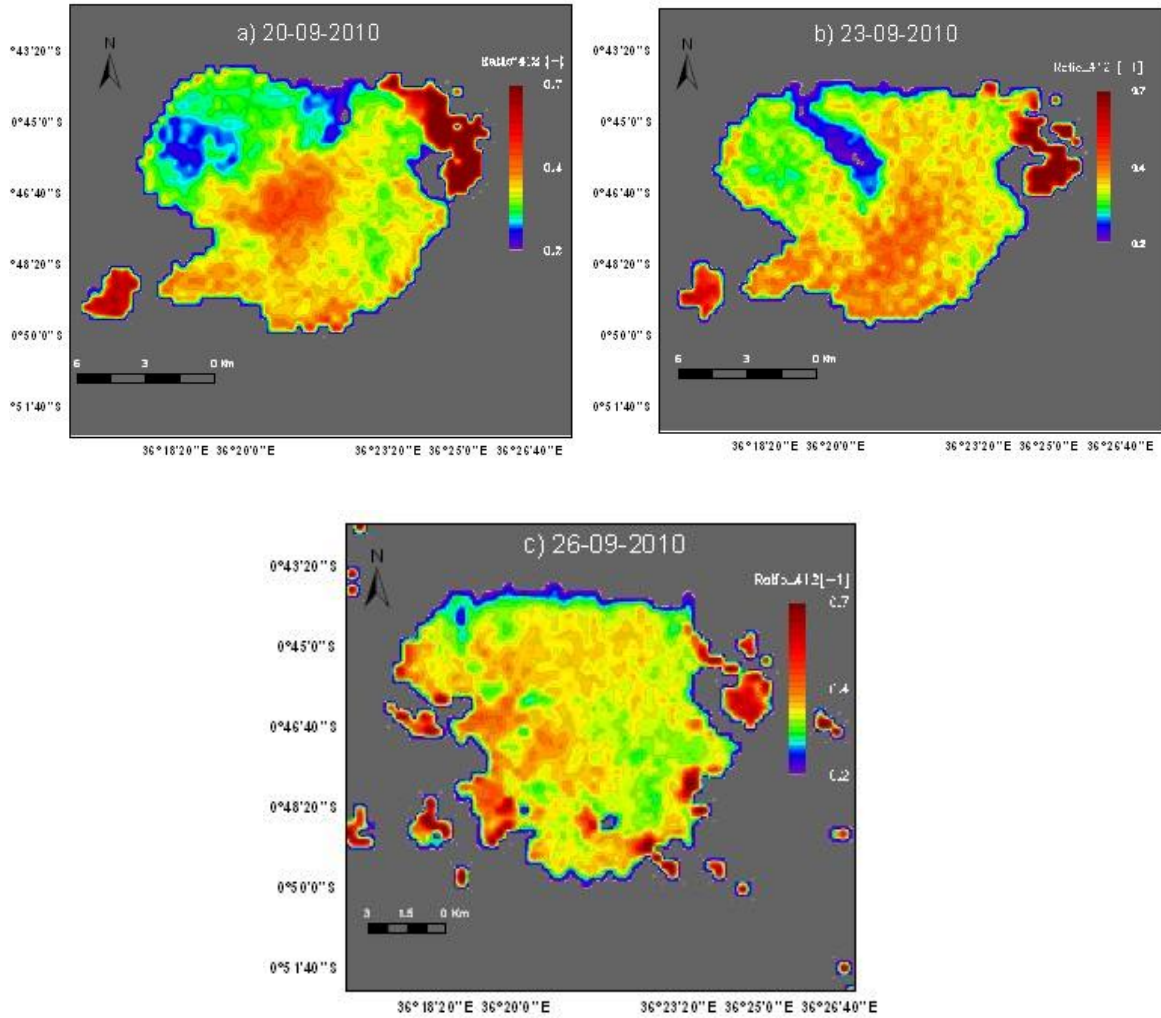
Figure 12: Spatial distribution of $a_{CDOM}/a_t(412)$ from MERIS acquired on a) 20 b) 23 c) 26 Sept 2010

4.5.   Variability of a_{CDOM}/a_t Ratio in Lake Naivasha

Monitoring the temporal and spatial dynamics of inland waters is essential for the understanding of inland water ecosystems. Monitoring the optical properties of local waters at several spatial and temporal scales can provide diagnostic information on natural and anthropogenic factors affecting the capacity of these waters to provide sufficient sunlight to planktons and macrophytes for photosynthesis and growth. CDOM absorption is strongly correlated with freshwater discharge as reported by Keith et al.(2002). Figure 12 illustrates the observed spatial variability of $a_{CDOM}/a_t(412)$ in the lake. The range of spatial variability of $a_{CDOM}/a_t(412)$ in the main lake is insignificant and frequency distribution is slightly flat compared with a normal distribution as shown in Figure 13(b). The frequency distribution shown in Figure 12(a) is resulted due to less absorptions of particles in the Crater lake $(a_P(412) = 3.52m^{-1})$ that increase the values of the ratio $(a_{CDOM}/a_t(412))$.
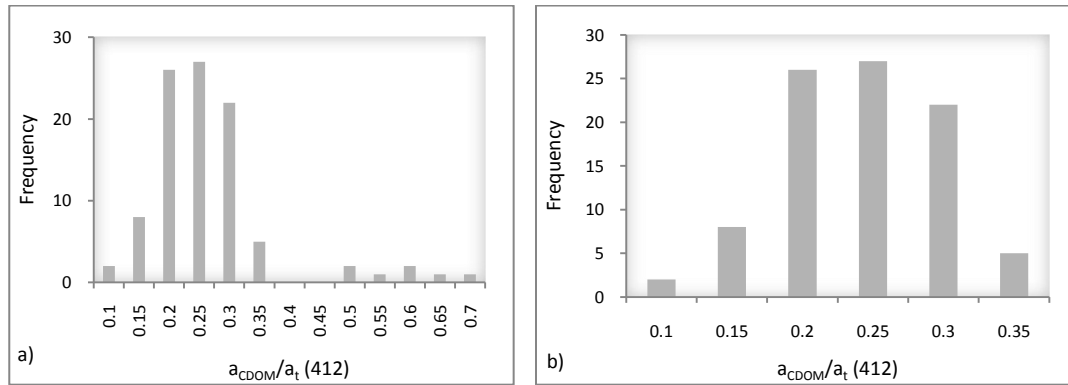
Figure 13: Variability of $a_{CDOM}/a_t(412)$ in a) lake Naivasha and b) Main lake

Apparent increases in absorptions of particles at Gilgil inlet and forest side region are associated with increases in wet season flow and water mix where surface runoff will deliver substantial quantities of terrestrial plant materials to the rivers and then to the lake Naivasha. The $a_{CDOM}/a_t(412)$ and $R_{rs}(555)$ values are inversely correlated, which indicates that $a_{CDOM}/a_t(412)$ increases as the turbidity decreases.
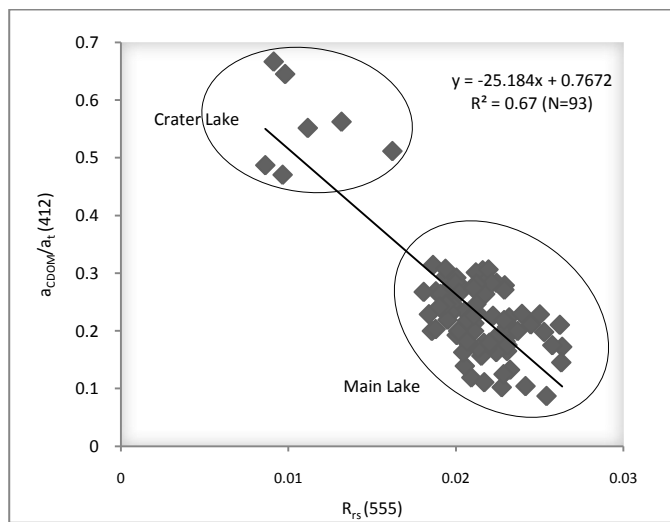
Figure 14: Inverse relationship of measured $a_{CDOM}/a_t(412)$ versus $R_{rs}(555)$

These higher values of $a_{CDOM}/a_t(412)$ reflect the absence of direct influence of river runoff and a relatively more important contribution of phytoplankton to total light absorption.

The variability of CDOM absorption is dependent on its sources (Section 2.3) and sinks (Section 2.4). If sources and sinks (removal) processes are in balance, the absorptive of CDOM may not vary considerably over time. The spatial variability of concentration of CDOM is insignificant in the lake Naivasha due to the fact that the size of the lake is small so that the CDOM introduced from the catchment can be distributed throughout the area by advection, diffusion, dispersion and flow-in. Table 1 and Figure 15 illustrate insignificance of the spatial variability of absorptions of CDOM with average value of 4.06 ± 0.63 m^{-1} and absorptions of CDOM is apparently high in Hippo pool region with average value of 4.46 ± 0.42 m^{-1} than in other regions; on the other hand, spatial variability of absorptions of particles in lake Naivasha are high with average value of 14.36 ± 5.51 m^{-1}.
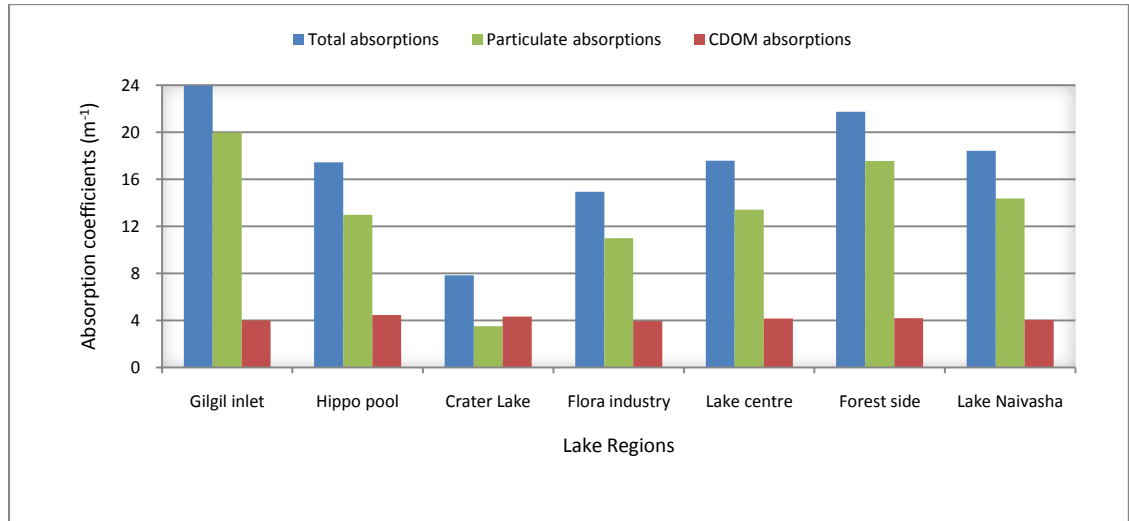
Figure 15: Absorption coefficients of lake Naivasha water constituents

On short terms, temporal differences of the water constituents in the lake Naivasha were observed for there was constant fluctuation of water color as observed during fieldwork especially in the main lake (Figure 8). Temporal differences that can be observed from Table 3 by focusing the monitoring time in short terms under less cloud coverage are an indication tool for presence of temporal variability of absorption coefficients of particles. This is because of inflowing from three perennial river systems, and smaller and seasonal streams into the lake that influences the concentration and distribution of nutrients and biochemical elements. Table 3 illustrates temporal differences that the range of temporal variability of $a_{CDOM}/a_t(412)$ is low; on the other hand, the temporal dynamics of absorptions of particles are apparently high. The spatial and temporal variability of the optical properties of CDOM in the lake water are, therefore, expected to be high during the spring-summer season when the photooxidation occurs and the river plume spreads over the lake. The values of $a_{CDOM}/a_t(412)$ increase in Crater lake, from 0.47 to 0.67. This may reflect the decreasing contribution of the terrigenous particles to the total light absorption in the surface waters when the particles gradually settle.

The $a_{CDOM}/a_t(412)$ decreases in the main lake with an average value of 0.22. These lower values probably reflect that the contribution of direct influence of river runoff and a relatively more important contribution to total light absorption.

Variations in reflectance of inland waters are primarily due to variations in turbidity (Sathyendranath et al., 1989). Subtle changes in the shape of the reflectance spectrum that may result from changes in the proportions of phytoplankton, CDOM and NAP are overwhelmed by the change in the magnitude of reflectance at all wavelengths due to variations in turbidity. This can clearly be observed from Figure 12(b) where after a rain event the inflow of the Giglil river has increased which increases incoming suspended particles load to the lake that in turn enhances the reflectance.

5.   CONCLUSIONS AND RECOMMENDATIONS

The absorptions and optical properties of CDOM in lake Naivasha were investigated from September 17 to October 3 in 2010. The results show that the spatial variability of absorption coefficients of CDOM is insignificant with average value of 4.06 $\pm$ 0.63 m^{-1} (Table 1; Figure 15).

The empirical algorithm developed for optically complex water is strong to quantify CDOM in Naivasha lake and its accuracy can be improved by minimizing the associated errors of in situ IOPs and spectra measurements. The measured spectra and absorptions of total and CDOM used as input for the empirical algorithm were often a source of error. Retrieved and measured a_{CDOM}/a_t at 412 nm provide good correlation ($R^2 = 0.81; p < 0.05$). The Root mean square error ($RMSE$) is less than 0.06.

The spectral slope of CDOM in the lake is 0.014 sr^{-1} which was computed from 93 samples collected from the lake at specific wavelengths. The values of a_{CDOM}/a_t at 412 nm for the whole lake varies between 0.09 and 0.67 with an average value of 0.24. The average value of a_{CDOM}/a_t at 412 nm is found to be 0.22 and 0.57 in main lake and Crater lake respectively. The values of $a_{CDOM}/a_t(412)$ in the Crater lake are high compared to the main lake due to less values of absorption coefficients of suspended particles.

Values retrieved from MERIS imageries correlate with value of $a_{CDOM}/a_t(412)$ measured during field campaign and hence, one can simply retrieve the value of absorption coefficients of CDOM in the lake from MERIS imageries by strategic sampling and improving laboratory measurement of total absorption coefficients of the lake Naivasha by using empirical algorithm proposed for optically complex water (Equation (11)).

CDOM concentrations are in general positively associated with flow up to the point. Hydrologic alterations that increase flow such as increased rainfall and basin releases in the lake watershed will increase CDOM concentrations up to a point. Although it follows that landuse changes that lead to increases in flow may in turn lead to increases in CDOM concentrations given sufficient source materials (Corbett et al., 2007). Long term temporal variations of CDOM concentrations and changes in its levels could be analyzed if images of the lake for past years would have been available. However, CDOM concentrations within the lake may be changing in concentration and temporally in view of the fact that basin releases due to erosion from unsustainable land use practices in its catchment and runoff from intensive horticultural industries are contributive to CDOM enrichment. Regular monitoring (e.g. once a month) would have been necessary if substantial temporal variations of water quality would be captured by in situ monitoring. If no substantial temporal differences are observed between satellite data and in situ data, satellite data can be used for time series analysis.

Optical properties of the surface waters are largely controlled by terrigenous inputs. The impact of the variations in the spectral shape of $a_{CDOM}(\lambda)$ and $a_P(\lambda)$ is relatively weak when CDOM dominates the total light absorption i.e. if $a_{CDOM}/a_t(412) > 0.70$. Particulate matter dominates the total light absorptions if $a_{CDOM}/a_t(412) < 0.60$ (Be´langer et al., 2008). This is because of the shallow depth of the lake allowing exposure to UV may allow photodegradation and less accumulation of CDOM. The spatial variability of absorption coefficient of CDOM was insignificant with average value of 4.06 $\pm$ 0.63. Absorption of particles in the lake varies between 2.30m^{-1} and 34.31m^{-1} with an average value of 14.36 m^{-1} and a standard deviation of 5.51 which confirms the large variability of $a_P(412)$ (phytoplankton and non algal particles) in the lake that influence the quality and quantity of subsurface irradiance in the Lake.

The main conclusions of this work are summarized as follow:
1.   The proposed model is simple and accurate and could be used for the Naivasha lake to quantify the contribution of CDOM to the total light absorption;
2.   The spectral slope of CDOM absorption can be considered constant with a value of 0.014 sr^{-1};
3.   A more pronounced spatial variability of CDOM was observed after rain events with particles playing the major roles in light absorption in the lake.

To enhance the efficiency of the algorithm the following recommendations should be considered:

- Accuracy can be increased by improving laboratory and optical measurements parallel with in situ measurement techniques for strategic sampling.
- Subsurface upwelling irradiance ($E_u(0^-\lambda)$) should be measured in order to exclude the actual values of water surface reflectances from remote sensing reflectances above water that are used as input in the retrieval of $a_{CDOM}/a_t(412)$.
- Movement of the boat and abundance of floating-leaved plants, *Nymphaea caerulea* should be avoided during optical measurements that bias the measurement values of spectra that in turn bias the values of coefficients of empirical algorithm. Establishing monitoring station to collect the spectra readings may resolve the aforesaid noises and avoid reflectances from floating vegetations in order to enhance the accuracy of spectra measurements.
- The spectral slope of CDOM values change with wavelength, and its covariance with season and CDOM concentration should be investigated by taking measurements in different seasons in order to determine the stable value of its spectral slope.

LIST OF REFERENCES

Abiya, I. O. (1996). Towards sustainable utilization of Lake Naivasha, Kenya. *Lakes & Reservoirs: Research and Management, 2*, 231-242.

Adams, J. A. Pecor, K. W. and Moore, P. A. (2009). Dissolved organic matter from elevated-CO2 detritus and its impact on the orientation of crayfish (Orconectes virilis) to a fish food source. *The North American Benthological Society, 28*(3), 638-648.

Aiken, G. R. McKnight, D. M. Wershaw, R. L. and MacCarthy, P. (1985). Humic substances In Soil, Sediment, and Water. *John Wiley & Sons.*

Babin, M. Stramski, D. Ferrari, G. M. Claustre, H. Bricaud, A. Obolensky, G. and Hoepffner, N. (2003b). Variations in the light absorption coefficients of phytoplankton, nonalgal particles, and dissolved organic matter in coastal waters around Europe. *Geophysical Research, 108*(C7), 3211.

Ballot, A. Kotut, K. Novelo, E. and Krienitz, L. (2009). Changes of phytoplankton communities in Lakes Naivasha and Oloidien, examples of degradation and salinization of lakes in the Kenyan Rift Valley. *Hydrobiologia, 632*, 359–363.

Be´langer, S. Babin, M. and Larouche, P. (2008). An empirical ocean color algorithm for estimating the contribution of chromophoric dissolved organic matter to total light absorption in optically complex waters. *Geophysical Research, 113*, C04027.

Becht, R. and Harper, D. M. (2002). Towards an understanding of human impact upon the hydrology of Lake Naivasha, Kenya. *Hydrobiologia, 488*, 1-11.

Blough, N. V. and Del Vecchio, R. (2002). Chromophoric DOM in the coastal environment. *Biogeochemistry of Marine Dissolved Organic Matter, D.A. Hansell and C.A. Carlson, eds., Academic Press, Cambridge, MA*, 509-546.

Chen, R. F. Bissett, P. Coble, P. Conmy, R. Bernard Gardner, G. Moran, M. A. Wang, X. Wells, M. L. Whelan, P. and Zepp, R. G. (2004). Chromophoric dissolved organic matter (CDOM) source characterization in the Louisiana Bight. *Marine Chemistry 89*, 257– 272.

Chuanmin, H. Zhongping, L. Frank, E. Muller-Karger Kendall, L. Carder and John, J., Walsh. (2006). Ocean Color reveals phase shift between marine plants and yellow substance. *IEEE Geoscience and Remote Sensing Letters, 3*(2), 262-266.

Corbett, C. A. Hilgendorf, M. B. Greenawalt-Boswell, J. Donley, L. Beever, L. B. and Recksiek, H. (2007). Colored dissolved organic matter (CDOM) workshop summary. *Charlotte Harbor National Estuary Program, Punta Gorda, Florida.*

Doxaran, D. Nagur C. Cherukuru Lavender, S. J. and Moore, G. F. (2004). Use of a Spectralon panel to measure the downwelling irradiance signal: case studies and recommendations. *Applied Optics, 43*(32), 5981-5986.

Everard, M. and Harper, D. M. (2002). Towards the sustainability of the Lake Naivasha Ramsar site and its catchment. *Hydrobiologia, 488*, 191–203.

Gallegos, C. L. and Neale, P. J. (2002). Partitioning spectral absorption in case 2 waters: discrimination of dissolved and particulate components. *Applied Optics, 41*(21), 4220-4233.

Giardino, C. Brando, V. E. Dekker, A. G. Strömbeck, N. and Candiani, G. (2007). Assessment of water quality in Lake Garda (Italy) using Hyperion. *Remote Sensing of Environment, 109*, 183–195.

Giardino, C. Bresciani, M. Pilkaityte, R. Bartoli, M. and Razinkovas, A. (2010). In situ measurements and satellite remote sensing of case 2 waters: first results from the Curonian Lagoon. *Oceanologia, 52*(2), 197-210.

Gordon, H. O. and Wang, M. (1994). Retrieval of water-leaving radiance and aerosol optical thickness over the oceans with SeaWiFS: A preliminary algorithm. *Appllied Optics, 33*, 443-452.

Green, S. and Blough, N. (1994). Optical absorption and fluorescence properties of chromophoric dissolved organic matter in natural waters. *Limnology and Oceanography, 39*(8), 1903–1916.

Hansell, D. A. and Carlson, C. A. (2002). Biogeochemistry of Marine Dissolved Organic Matter. *1st edition, Academic Press, San Diego, California.*

Harper, D. (1992). The ecological relationships of aquatic plants at Lake Naivasha, Kenya. *Hydrobiologia, 232*, 65-71.

Harper, D. M. (2006). The sacrifice of Lake Naivasha. *Swara, East African Wild Life Society, 29*, 28-37.

Harper, D. M. Adams, C. and Mavuti, K. (1995). The aquatic plant communities of the Lake Naivasha wetland, Kenya: pattern, dynamics and conservation. *Wetlands Ecology and Management, 3*(2), 111-123.

Harper, D. M. Mavuti, K. M. and Muchiri, S. M. (1990). Ecology and Management of Lake Naivasha, Kenya, in Relation to Climatic Change, Alien Species' Introductions, and Agricultural Development. *Environmental Conservation, Cambridge University Press, 17*, 328-336.

Harvey, G. R. Boran, D. A. Piotrowicz, S. R. and Weisel, C. P. (1984). Synthesis of marine humic substances from unsaturated lipids. *Nature, 309*(5965), 244-246.

Henderson, I. F. (1979). Henderson's Dictionary of Biological Terms. *Longman Science & Technology, 9 edition.*

Keith, D. J. Yoder, J. A. and Freeman, S. A. (2002). Spatial and Temporal Distribution of Coloured Dissolved Organic Matter (CDOM) in Narragansett Bay, Rhode Island: Implications for Phytoplankton in Coastal Waters. *Estuarine, Coastal and Shelf Science, 55*, 705–717.

Kilham, P. and Kilham, S. S. (1990). Endless summer: internal loading processes dominate nutrient cycling in tropical lakes. *Freshwat. Biol., 23*, 379–389.

Kirk, J. T. O. (1994). Light and Photosynthesis in Aquatic Ecosystems. *2nd edition. Cambridge University Press, Cambridge, U.K.*

Kitaka, N. Harper, D., M. and Mavuti, K. M. (2002). Phosphorus inputs to Lake Naivasha, Kenya, from its catchment and the trophic state of the lake. *Hydrobiologia, 488*, 73–80.

Kracht, O. and Gleixner, G. (2000). Isotope analysis of pyrolysis products from Sphagnum peat and dissolved organic matter from bog water. *Organic Geochemistry, 31*, 645-654.

Laanen, M. L. (2007). Yellow Matters: Improving the remote sensing of Coloured Dissolved Organic Matter in inland freshwaters. *Ph.D. dissertation Vrije Universiteit Amsterdam, The Netherlands.*

Lee, Z. and Carder, K. (2005). Hyperspectral remote sensing. *Remote Sensing of Coastal Aquatic Environments*, 181–204.

Lee, Z. Carder, K. Arnone, R. and He, M. (2007). Determination of Primary Spectral Bands for Remote Sensing of Aquatic Environments. *Sensors, 7*, 3428-3441.

Maritorena, S. Siegel, D. and Peterson, A. (2002). Optimization of a semianalytical ocean color model for global-scale applications. *Appllied Optics, 41*, 2705–2714.

McKnight, D. M. and Aiken, G. R. (1998). Sources and age of aquatic humic substances. *Ecology and Biogeochemistry of Marine Dissolved Organic Matter*, 9-39.

McPherson, B. F. and Miller, R. L. (1994). Causes of light attenuation in Tampa Bay and Charlotte Harbor. *Water Resources Bulletin, 30*(1), 43-53.

Mobley, C. D. (1999). Estimation of the remote-sensing reflectances from above-water measurements. *Appl. Opt, 38*, 7442–7455.

Mueller, J. L. Davis, C. Arnone, R. Frouin, R. Carder, K. L. Lee, Z. P. Steward, R. G. Hooker, S. and Mobley, C. D. (2002). Above-water radiance and remote sensing reflectance measurement and analysis protocols; in Ocean Optics Protocols for Satellite Ocean Color Sensor Validation. *Revision 3, NASA/TM-2002-210004, Ed. by J. L. Mueller and G. S. Fargion*, 171-182.

Mulholland, P. J. (2003). Large-scale patterns in dissolved organic carbon concentration, flux and sources. *In S. E. G. Findlay and R. L. Sinsabaugh (eds.), Aquatic Ecosystems: Interactivity of Dissolved Organic Matter. Aquatic Ecology Series, Academic Press, San Diego, California*, 139–160.

Muller, F. L. L. Larsen, A. Stedmon, C. A. and Sondergaard, M. (2005). Interactions between algal/bacterial populations and trace metals in fjord surface waters during a nutrient-stimulated summer bloom. *Limnology and Oceanography, 50*, 1855–1871.

Nelson, N. B. and Siegel, D. A. (2002). Chromophoric DOM in Open Ocean. *Biogeochemistry of Marine Dissolved Organic Matter*, 547-578.

Nieke, B. Reuter, R. Heuermann, R. Wang, H. Babin, M. and Therriault, J. C. (1997). Light Absorption and fluorescence properties of chromophoric dissolved organic matter (CDOM), in the St. Lawrence Estuary (Case 2 waters). *Continental Shelf Research, 17*(3), 235-252.

O'Reilly, J. F. Maritorena, S. Mitchell, B. G. Siegel, D. A. Garver, S. A. and Kahru, M. (1998). Ocean color chlorophyll algorithms for SeaWiFS. *J.Geophys.Res, 103*, 24891-24900.

Obernoster, I. Ruardij, P. and Herndl, G. J. (2001). Spatial and diurnal dynamics of dissolved organic matter (DOM) fluorescence and H_2O_2 and the photochemical oxygen demand of surface water DOM across the subtropical Atlantic Ocean. *Limnology and Oceanography, 46*, 632-643.

Salama, M. S. Dekker, A. Su, Z. Mannaert, C. M. and Verhoef, W. (2009). Deriving inherent optical properties and associated inversion-uncertainties in the Dutch Lakes. *Hydrology and Earth System Sciences, 13*, 1113–1121.

Salas, H. J. and Martino, P. (1991). A simplified phosphorus trophic state model for warm-water tropical lakes. *Water Research, 25*, 341–350.

Sathyendranath, S. Prieur, L. and Morel, A. (1989). A three-component model of ocean colour and its application to remote sensing of phytoplankton pigments in coastal waters. *International Journal of Remote Sensing, 10*(8), 1373–1394.

Singer, P. C. (1999). Formation and control of disinfection by-products in drinking water. *American Water Works Association, Denver, CO.*

Stedmon, C. A. and Markager, S. (2005). Resolving the compositional changes in dissolved organic matter (DOM) in a temperate estuary and its catchment, using spectrofluorometry and PARAFAC analysis. *Limnology & Oceanography, 50*(2), 686-697.

Stedmon, C. A. Markager, S. Sondergaard, M. Vang, T. Laubel, A. Borch, N. H. and Windelin, A. (2006). Dissolved organic matter (DOM) export to a temperate estuary seasonal variations and implications of land use. *Estuaries and Coasts, 29*(3), 388-400.

Stedmon, C. A. and Osburn, C. L. (2006). Quantitative and Qualitative Prediction of Light Absorption by Colored Dissolved Organic Matter in the Coastal Zone. *Dept. Marine Ecology, National Environmental Research Institute (NERI), Denmark.*

Steinberg, C. E. W. (2003). Ecology of Humic Substances in Freshwater. *1 ed. Springer.*

Tilstone, G. H. Moore, G. F. Sørensen, K. Röttgers, R. Jørgensen, P. V. Vicente, V. M. and Ruddick, K. G. (2002). Regional Validation of MERIS Chlorophyll products in North Sea coastal waters. *REVAMP Inter-calibration Report*, 18-20.

Vincent Davies, C. T. and Beresford, A. (1979). Recent changes in the level of Lake Naivasha, Kenya, as an indicator of equatorial westerlies over East Africa. *Climate Change 2*, 175-189.

Wells, M. L. (2001). Marine colloids and trace metals. *In D. A. Hansell and C. A. Carlson (eds.), Biogeochemistry of Marine Dissolved Organic Matter. Academic Press, San Diego, California*, 367–404.

Yee, L. F. Abdullah, M. P. Ata, S. and Ishak, B. (2006). Dissolved organic matter and its impact on the chlorine demand of treated water. *The Malaysian Journal of Analytical Sciences, 10*(2), 243-250.